Fast identification of cracks using higher-order topological sensitivity for 2-D potential problems

Marc Bonnet

Fast identification of cracks using higher-order topological sensitivity for 2-D potential problems

Marc BONNET

Solid Mechanics Laboratory (UMR CNRS 7649), Department of Mechanics
École Polytechnique, F-91128 Palaiseau cedex, France
bonnet@lms.polytechnique.fr

Abstract

This article concerns an extension of the topological sensitivity (TS) concept for 2D potential problems involving insulated cracks, whereby a misfit functional J is expanded in powers of the characteristic size a of a crack. Going beyond the standard TS, which evaluates (in the present context) the leading $O(a^2)$ approximation of J, the higher-order TS established here for a small crack of arbitrarily given location and shape embedded in a 2-D region of arbitrary shape and conductivity yields the $O(a^4)$ approximation of J. Simpler and more explicit versions of this formulation are obtained for a centrally-symmetric crack and a straight crack. A simple approximate global procedure for crack identification, based on minimizing the $O(a^4)$ expansion of J over a dense search grid, is proposed and demonstrated on a synthetic numerical example. BIE formulations are prominently used in both the mathematical treatment leading to the $O(a^4)$ approximation of J and the subsequent numerical experiments.

1 INTRODUCTION

The sensitivity analysis of objective functions has a firm mathematical basis and provides efficient computational tools for e.g. optimal design or inversion of experimental data. Along with classical sensitivity methods, performing first-order perturbation analyses with respect to small variations of some feature of the system under consideration, another sensitivity concept, namely that of topological sensitivity, appeared more recently in the context of topological optimization of mechanical structures [14, 26]. Topological sensitivity is concerned with quantifying the perturbation of an objective function J with respect to the nucleation of a small object $D_a(\boldsymbol{z})$ of characteristic linear size a and specified location $\boldsymbol{z}$, as a function of $\boldsymbol{z}$. Denoting by $J(a;\boldsymbol{z})$ the value achieved by J when $D_a(\boldsymbol{z})$ is the only perturbation to an otherwise known reference medium, then in 2-D situations with Neumann or transmission conditions on $\partial D_a(\boldsymbol{z})$ the topological derivative $\mathcal{T}_2(\boldsymbol{z})$ appears through an expansion of the form

$$J(a;\boldsymbol{z}) = J(0) + a^2\mathcal{T}_2(\boldsymbol{z}) + o(a^2).$$

Subsequent investigations have also established the usefulness of the topological sensitivity as a preliminary sampling tool for defect identification problems, providing estimates of location, size and number of a set of sought defects [6, 10, 15, 18, 19, 21, 22]. This approach has also been extended by formulating higher-order expansions of $J(a;\boldsymbol{z})$. The $O(a^4)$ expansion of cost functionals involving the solution of a 2-D potential problem in a domain of arbitrary shape containing a small inclusion of size a, of the form

$$J(a;\boldsymbol{z}) = J(0) + \mathcal{T}_2(\boldsymbol{z})a^2 + \mathcal{T}_3(\boldsymbol{z})a^3 + \mathcal{T}_4(\boldsymbol{z})a^4 + o(a^4) \equiv J(0) + J_4(a;\boldsymbol{z}) + o(a^4), \qquad (1)$$

where coefficients $\mathcal{T}_2, \mathcal{T}_3, \mathcal{T}_4$ depend on the assumed characteristics of the small nucleating object, is established in [9] (for arbitrary cost functionals expressed as boundary integrals and inclusions of arbitrary shape) and [25] (for potential energy and circular inclusions), while similar expansions for the scattering by sound-hard obstacles are established in [8] for problems governed by the 3-D Helmholtz equation. The concept of topological sensitivity, and higher-order topological expansions such as (1), are particular instances of the broader class of asymptotic methods, where approximate

solutions to problems featuring a small geometrical parameter a are sought in the form of expansions with respect to a, see e.g. [2, 23].

This article is a continuation of [9] where the small nucleating object is a perfectly-insulating crack, through which discontinuities of the potential are allowed. Its aim is twofold: (i) to establish the expressions of coefficients $\mathcal{T}_2, \mathcal{T}_3, \mathcal{T}_4$ for a crack of size a embedded in a 2-D medium characterized by a scalar conductivity, permitting computationally efficient methods for evaluating small-crack expansions of cost functionals, and (ii) to demonstrate the effectiveness of the resulting expansion (1) for crack identification purposes. Since the sensitivity of cost functionals (rather than field variables) is emphasized here, an adjoint solution-based approach is formulated as it avoids the (involved and costly) evaluation of higher-order sensitivities of field variables, following what is now common practice in usual sensitivity analyses and previous works on topological sensitivity [3, 6, 9, 10, 16, 22]. Coefficients $\mathcal{T}_2, \mathcal{T}_3, \mathcal{T}_4$ are hence found to be expressed in terms of the free and adjoint fields (i.e. the response of the reference medium to the applied and adjoint excitations), and also (for $\mathcal{T}_4$) on the Green's function associated with the geometry and boundary condition structure under consideration. The formal analysis presented herein is quite similar in its principle to that of [9], which can indeed be considered as generic, although the mathematical details of the present and former analyses are quite different.

Then, adapting the approach developed in [9] for inclusion identification, the functions $\mathcal{T}_2, \mathcal{T}_3, \mathcal{T}_4$ can be computed for sampling points $\boldsymbol{z}$ spanning a search grid at a computational cost commensurate to a small number of forward solutions in the reference medium, allowing to set up a computationally fast approximate global identification procedure where the polynomial approximant $J_4(a; \boldsymbol{z})$ of J is minimized w.r.t. a for a large number of trial crack locations $\boldsymbol{z}$. In comparison, usual global search methods such as evolutionary algorithms [24] or parameter-space sampling methods [28] are much more computation-intensive as they require large numbers of evaluations of J.

This article is organized as follows. Formulations and notation for the forward problems of interest and cost functionals are reviewed in Sec. 2. Then, general expressions for coefficients $\mathcal{T}_2, \mathcal{T}_3, \mathcal{T}_4$ are established for a small crack of arbitrary shape buried in an arbitrary domain (Sec. 5), based on a methodology whose main components are an adjoint-solution framework (Sec. 3) and an expansion of the total field on the crack (Sec. 4). Simpler formulae are next obtained for the useful special case of a centrally-symmetric crack (Sec. 5.2), leading to explicit formulae for a straight crack (section 5.3). The approximate global search procedure for crack identification based on $J_4(a; \boldsymbol{z})$ is presented and applied on a synthetic crack identification problem in Sec. 6.

2 FORWARD PROBLEM AND MISFIT FUNCTIONALS

Reference configurations of interest here consist of a two-dimensional domain Ω, either bounded or unbounded, with a sufficiently regular boundary S, and filled with a isotropic medium characterized by a constant scalar conductivity k. Defects are here considered in the form of perfectly-insulating cracks, modelled by a (possibly curved and not simply-connected) line D through which the potential u is allowed to jump while its normal derivative is zero on the two faces $D^{\pm}$.

2.1 Forward problem

Let D denote a trial crack and $\Omega_D = \Omega \setminus D$ the corresponding cracked domain. The application of prescribed potential u^{d} and flux p^{d} over S_{u} and S_{p}, respectively (where S_{p} and S_{u} are complementary disjoint subsets of S) give rise to the potential u_D in Ω_D, governed by the field equation

$$\mathrm{div}(k\boldsymbol{\nabla} u_D) = 0 \quad (\text{in } \Omega_D) \tag{2}$$

and the boundary conditions

$$\text{(a) } u_D = u^{\mathrm{d}} \quad (\text{on } S_{\mathrm{u}}), \qquad \text{(b) } p[u_D] = p^{\mathrm{d}} \quad (\text{on } S_{\mathrm{p}}), \qquad \text{(c) } p^{\pm}[u_D] = 0 \quad (\text{on } D^{\pm}) \tag{3}$$

(where $D^{\pm}$ denote the two crack faces, $w \mapsto p[w] = k\boldsymbol{\nabla} w \cdot \boldsymbol{n}$ and $w \mapsto p[w] = k\boldsymbol{\nabla} w \cdot \boldsymbol{n}^{\pm}$ respectively denote the flux operator on S and $D^{\pm}$, and with the unit normals $\boldsymbol{n}$ to S and $\boldsymbol{n}^{\pm}$ to $D^{\pm}$ directed

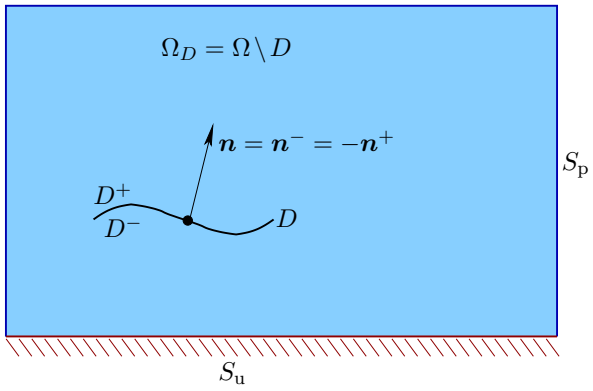

Figure 1: *Forward problem: geometry and notations.*

outwards of Ω), see Fig. 1). In addition, the *free field* u is defined as the solution to the boundary-value problem

$$\mathrm{div}(k\boldsymbol{\nabla} u) = 0 \ \ (\text{in } \Omega), \qquad p[u] = p^\mathrm{d} \ \ (\text{on } S_\mathrm{p}), \qquad u = u^\mathrm{d} \ \ (\text{on } S_\mathrm{u}), \tag{4}$$

i.e. is the potential arising in Ω for the same boundary data $p^\mathrm{d}, u^\mathrm{d}$ in the absence of any crack.

The following reciprocity identity is now provided for later convenience.

Lemma 1. *Let u_D verify (2) and (3c), and let w be any trial field verifying div$(k\boldsymbol{\nabla} w) + b = 0$ in Ω (with b denoting a given source distribution) and such that $[\![w]\!] = 0$, $p^+[w] + p^-[w] = 0$ on D (where $[\![f]\!] = f^+ - f^-$ denotes the jump of f across D). The following reciprocity identity holds true:*

$$\int_S \big[p[w]u_D - p[u_D]w\big]\, ds + \int_{\Omega_D} bu_D\, dV - \int_D p[w][\![u_D]\!]\, ds = 0, \tag{5}$$

where the flux operator $p[\cdot]$ on D is defined in terms of the unit normal $\boldsymbol{n} = \boldsymbol{n}^-$ (i.e. $p[\cdot] = p^-[\cdot]$).

Proof. Identity (5) follows directly from the third Green's formula

$$\int_{\mathcal{O}} \big[w\Delta u_D - u_D \Delta w\big]\, \mathrm{d}V + \int_{\partial\mathcal{O}} \big[(\boldsymbol{\nabla} w \cdot \boldsymbol{n})u_D - (\boldsymbol{\nabla} u_D \cdot \boldsymbol{n})w\big]\, \mathrm{d}s = 0, \tag{6}$$

written for $\mathcal{O} = \Omega_D$, $\partial\mathcal{O} = S \cup D$ and the assumed conditions for u_D and w on D. □

2.2 Misfit functionals

Considering the problem of identifying an unknown crack D^true from supplementary data consisting of measured values u^obs of the potential and p^obs of the flux, collected respectively on S_p and S_u (or subsets thereof), the misfit between observations $u^\mathrm{obs}, p^\mathrm{obs}$ and their predictions $u_D, p_D = p[u_D]$ for a trial crack D may be expressed through a cost functional of format

$$\mathcal{J}(D) = \int_{S_\mathrm{p}} \varphi_\mathrm{p}\big(u_D(\boldsymbol{\xi}), \boldsymbol{\xi}\big)\, \mathrm{d}s(\boldsymbol{\xi}) + \int_{S_\mathrm{u}} \varphi_\mathrm{u}\big(p_D(\boldsymbol{\xi}), \boldsymbol{\xi}\big)\, \mathrm{d}s(\boldsymbol{\xi}). \tag{7}$$

For instance, the commonly-used output least-squares misfit functional $\mathcal{J}_\mathrm{LS}(D)$ corresponds to

$$\varphi_\mathrm{p}\big(u_D(\boldsymbol{\xi}), \boldsymbol{\xi}\big) = \frac{1}{2}\big|u_D(\boldsymbol{\xi}) - u^\mathrm{obs}(\boldsymbol{\xi})\big|^2, \quad \varphi_\mathrm{u}\big(p_D(\boldsymbol{\xi}), \boldsymbol{\xi}\big) = \frac{1}{2}\big|p_D(\boldsymbol{\xi}) - p^\mathrm{obs}(\boldsymbol{\xi})\big|^2. \tag{8}$$

Suitably modified definitions of φ_u and φ_p easily allow to accommodate data available on subsets of S_u or S_p, including discrete data. Moreover, the generic format (7) may be used for other purposes, e.g. expressing the potential energy of the cracked body by setting

$$\varphi_\mathrm{p}\big(u_D(\boldsymbol{\xi}), \boldsymbol{\xi}\big) = -\frac{1}{2}p^\mathrm{d}(\boldsymbol{\xi})u_D(\boldsymbol{\xi}), \quad \varphi_\mathrm{u}\big(p_D(\boldsymbol{\xi}), \boldsymbol{\xi}\big) = \frac{1}{2}p_D(\boldsymbol{\xi})u^\mathrm{d}(\boldsymbol{\xi}). \tag{9}$$

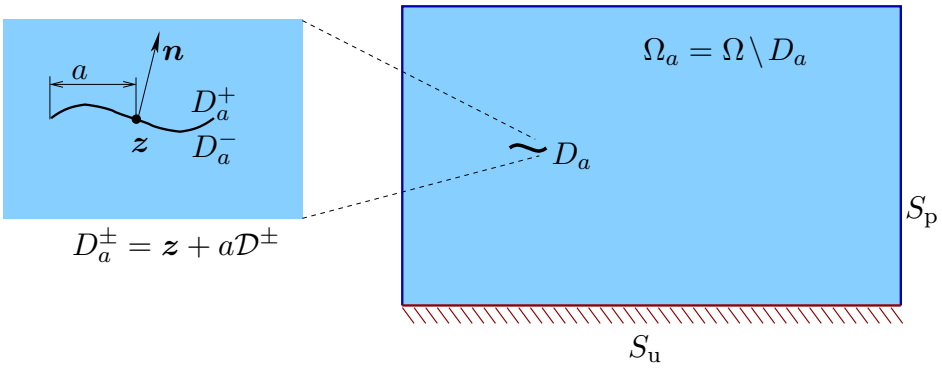

Figure 2: *Small-crack asymptotics: geometry and notations.*

In what follows, attention will focus on the case of trial cracks of small linear size a and specified location and shape. The main objectives of this article are (i) to establish an expansion of cost functionals of format (7) with respect to a, whose coefficients depend on the crack location $\boldsymbol{z}$, and (ii) to formulate and demonstrate a computationally fast approximate global search method for crack identification exploiting such expansions for misfit functionals.

3 ADJOINT SOLUTION APPROACH FOR EXPANSION OF MISFIT FUNCTIONAL

Let $D_a(\boldsymbol{z}) = \boldsymbol{z} + a\mathcal{D}$, where $\mathcal{D} \subset \mathbb{R}^2$ is a fixed open curve of length $|\mathcal{D}|$ and centered at the origin, define a crack of (small) size $a > 0$ centered at a specified location $\boldsymbol{z} \in \Omega$ (Fig. 2). The crack shape is hence specified through the choice of normalized crack $\mathcal{D}$ (e.g. $\mathcal{D}$ is a segment of unit half-length for a small straight crack). The cracked domain is then $\Omega_a(\boldsymbol{z}, \mathcal{D}) = \Omega \setminus D_a(\boldsymbol{z})$.

One is here concerned with small-crack approximations of cost functionals (7). Accordingly, let $u_a(\cdot; \boldsymbol{z})$ denote the solution to equations (2), (3) with $D = D_a(\boldsymbol{z})$, and define $J(a; \boldsymbol{z})$ by

$$J(a; \boldsymbol{z}) = \mathcal{J}\big(D_a(\boldsymbol{z})\big) = \int_{S_\mathrm{p}} \varphi_\mathrm{p}(u_a(\boldsymbol{\xi}), \boldsymbol{\xi})\, \mathrm{d}s(\boldsymbol{\xi}) + \int_{S_\mathrm{u}} \varphi_\mathrm{u}(p_a(\boldsymbol{\xi}), \boldsymbol{\xi})\, \mathrm{d}s(\boldsymbol{\xi}), \tag{10}$$

with $p_a \equiv p[u_a]$. For notational convenience, explicit references to $\boldsymbol{z}$ will often be omitted in the sequel, e.g. by writing $J(a)$ or $u_a(\boldsymbol{\xi})$ instead of $J(a; \boldsymbol{z})$ or $u_a(\boldsymbol{\xi}; \boldsymbol{z})$.

3.1 Expansion of misfit functional based on adjoint solution

Let v_a denote the perturbation of the potential caused by a small crack nucleating at $\boldsymbol{z}$, i.e.:

$$v_a = u_a - u \qquad (\text{in } \Omega_a), \tag{11}$$

noting for later reference that v_a verifies homogeneous boundary conditions (wherein $q_a \equiv p[v_a]$):

$$\text{(a)}\ \ q_a = 0\ \ (\text{on } S_\mathrm{p}), \qquad \text{(b)}\ \ v_a = 0\ \ (\text{on } S_\mathrm{u}), \qquad \text{(c)}\ \ q_a^\pm = \mp p[u]\ \ (\text{on } D_a^\pm). \tag{12}$$

Since (i) the previously-known topological sensitivity of J is established on the basis of an expansion of (10) to first order in (v_a, q_a), and (ii) cost functions with quadratic dependence on $(u_D, p[u_D])$ are often considered in applications (e.g. for identification purposes), it is natural to seek a polynomial approximation of $J(a)$ by exploiting a second-order expansion of (10) in (v_a, q_a), i.e.:

$$J(a) = J(0) + \int_{S_\mathrm{p}} \varphi_\mathrm{p}'\, v_a\, \mathrm{d}s + \int_{S_\mathrm{u}} \varphi_\mathrm{u}'\, q_a\, \mathrm{d}s + \frac{1}{2}\int_{S_\mathrm{p}} \varphi_\mathrm{p}''\, v_a^2\, \mathrm{d}s + \frac{1}{2}\int_{S_\mathrm{u}} \varphi_\mathrm{u}''\, q_a^2\, \mathrm{d}s + o\big(\|v_a\|^2_{L^2(S_\mathrm{p})}, \|q_a\|^2_{L^2(S_\mathrm{u})}\big), \tag{13}$$

where $\|w\|_{L^2(S)}$ denotes the L^2-norm of w on surface S, and having set

$$\varphi'_{\rm p} = \frac{\partial \varphi_{\rm p}}{\partial u_a}\Big|_{u_a=u}, \quad \varphi'_{\rm u} = \frac{\partial \varphi_{\rm u}}{\partial p_a}\Big|_{p_a=p}, \quad \varphi''_{\rm p} = \frac{\partial^2 \varphi_{\rm p}}{\partial u_a^2}\Big|_{u_a=u}, \quad \varphi''_{\rm u} = \frac{\partial^2 \varphi_{\rm u}}{\partial p_a^2}\Big|_{p_a=p}. \tag{14}$$

In particular, the above quantities are given by

$$\varphi'_{\rm p} = u - u^{\rm obs}, \quad \varphi'_{\rm u} = p - p^{\rm obs}, \quad \varphi''_{\rm p} = 1, \quad \varphi''_{\rm u} = 1 \tag{15}$$

for $\varphi_{\rm p}, \varphi_{\rm u}$ defined by (8), and

$$\varphi'_{\rm u} = \frac{1}{2}u^{\rm d}, \quad \varphi'_{\rm p} = -\frac{1}{2}p^{\rm d}, \quad \varphi''_{\rm u} = 0, \quad \varphi''_{\rm p} = 0 \tag{16}$$

for $\varphi_{\rm p}, \varphi_{\rm u}$ defined by (9). Moreover, expansion (13) is exact, i.e. has a zero remainder, in both cases.

Lemma 2 (reformulation of misfit functional expansion using an adjoint solution). *Let the* adjoint field $\hat{u}$ *be defined as the solution of the adjoint problem*

$$\textit{(a)}\ \ k\Delta\hat{u} = 0\ \ (\textit{in}\ \Omega)\,, \quad \textit{(b)}\ \ p[\hat{u}] = \varphi'_p\ \ (\textit{on}\ S_p)\,, \quad \textit{(c)}\ \ \hat{u} = -\varphi'_u\ \ (\textit{on}\ S_u). \tag{17}$$

Expansion (13) then admits the alternative form (wherein $\phi_a \equiv [\![u_a]\!]$)

$$J(a) = J(0) + \int_{D_a} p[\hat{u}]\phi_a \, ds + \frac{1}{2}\int_{S_p} \varphi''_p \, v_a^2 \, ds + \frac{1}{2}\int_{S_u} \varphi''_u \, q_a^2 \, ds + o(\|v_a\|^2_{L^2(S_p)}, \, \|q_a\|^2_{L^2(S_u)}). \tag{18}$$

Proof. Invoking reciprocity identity (5) with $w = \hat{u},\ b = 0$ and boundary conditions (12) and (17b,c) and noting that

$$\int_{S_{\rm p}} \varphi'_{\rm p} \, u \, {\rm d}s + \int_{S_{\rm u}} \varphi'_{\rm u} \, p[u] \, {\rm d}s = 0$$

by virtue of $u, \hat{u}$ both being harmonic in Ω, one obtains identity

$$\int_{S_{\rm p}} \varphi'_{\rm p} \, v_a \, {\rm d}s + \int_{S_{\rm u}} \varphi'_{\rm u} \, q_a \, {\rm d}s = \int_{D_a} p[\hat{u}]\phi_a \, {\rm d}s$$

which, inserted into expansion (13), yields the desired reformulation (18). □

3.2 Previous results on topological sensitivity for crack problems

The leading contribution to $J(a)$ in the small-crack limit has been found in [4], on the basis of identity (18) truncated to first order in (v_a, q_a) (i.e. without the last two integrals), to be given by

$$J(a) = J(0) + a^2 \mathcal{T}_2(\boldsymbol{z}; \mathcal{D}) + o(a^2) \tag{19}$$

in terms of the *topological derivative* $\mathcal{T}_2$, given in the present context of 2-D potential problems by

$$\mathcal{T}_2(\boldsymbol{z}; \mathcal{D}) = \boldsymbol{\nabla}\hat{u}(\boldsymbol{z}) \cdot \boldsymbol{\mathcal{A}}_{11}(\mathcal{D}) \cdot \boldsymbol{\nabla} u(\boldsymbol{z}), \tag{20}$$

where the second-order tensor $\boldsymbol{\mathcal{A}}_{11}(\mathcal{D})$, known as '(first) polarization tensor', has been established for any crack shape $\mathcal{D}$ in [4] (see Eq. (48)). For the simplest case of a straight crack, where $\mathcal{D}$ is a line segment with length 2 and unit normal $\boldsymbol{n}$, one has the explicit expression

$$\boldsymbol{\mathcal{A}}_{11}(\mathcal{D}) = k\pi \boldsymbol{n} \otimes \boldsymbol{n}. \tag{21}$$

Moreover, the leading asymptotic behaviour of the perturbed field is characterized by

$$v_a(\boldsymbol{x}; \boldsymbol{z}) = a^2 W(\boldsymbol{x}; \boldsymbol{z}) + o(a^2), \qquad q_a(\boldsymbol{x}; \boldsymbol{z}) = a^2 p[W](\boldsymbol{x}; \boldsymbol{z}) + o(a^2) \qquad (\boldsymbol{x} \in S) \tag{22}$$

on the external boundary, and by

$$\phi_a(\boldsymbol{x}; \boldsymbol{z}) = a V_1\big((\boldsymbol{x} - \boldsymbol{z})/a\big) + o(a) \qquad (\boldsymbol{x} \in D_a) \tag{23}$$

on D_a, where the functions W and V_1 are known and depend on $\mathcal{D}$ (see Eqs. (53) and (45a)).

3.3 Derivation of expansion of $J(a)$: methodology and notation

To incorporate the effect of the leading contribution as $a \to 0$ of the quadratic terms v_a^2 and q_a^2 in the asymptotic analysis, an expansion of $J(a)$ must, in view of (18) and (22), be performed to order $O(a^4)$ at least. As (18) involves integrals over the vanishing crack D_a, the position vector $\bar{\boldsymbol{\xi}} \in D_a$ is scaled for this purpose according to:

$$\boldsymbol{\xi} = \boldsymbol{z} + a\bar{\boldsymbol{\xi}} \qquad (\boldsymbol{\xi} \in D_a,\, \bar{\boldsymbol{\xi}} \in \mathcal{D}). \tag{24}$$

In particular, this mapping transforms integrals over D_a into integrals over $\mathcal{D}$, with the differential length element rescaled according to

$$\mathrm{d}s(\boldsymbol{\xi}) = a\, \mathrm{d}s(\bar{\boldsymbol{\xi}}) \quad (\boldsymbol{\xi} \in D_a,\, \bar{\boldsymbol{\xi}} \in \mathcal{D}) \tag{25}$$

In view of (18), (22) and (25), establishing the sought $O(a^4)$ expansion of $J(a)$ requires a $O(a^3)$ expansion of ϕ_a on D_a. The previously known leading behavior (23) suggests to seek an asymptotic expression of ϕ_a of the form

$$\phi_a(\boldsymbol{\xi}) = aV_1(\bar{\boldsymbol{\xi}}) + a^2V_2(\bar{\boldsymbol{\xi}}) + \frac{a^3}{2}V_3(\bar{\boldsymbol{\xi}}) + o(a^3) \qquad (\boldsymbol{\xi} \in D_a,\, \bar{\boldsymbol{\xi}} \in \mathcal{D}), \tag{26}$$

where V_1, V_2, V_3 are functions defined on $\mathcal{D}$, which have to be determined in order to formulate an explicit expression for the expansion of $J(a)$. This task, based on expanding about $a = 0$ an integral equation formulation for ϕ_a, is now addressed.

4 EXPANSION OF FIELD ON THE CRACK

4.1 Integral equation formulation of the forward crack problem

Let the Green's function $\mathcal{G}(\boldsymbol{x}, \boldsymbol{\xi})$ associated with the domain Ω and partition $S = S_\mathrm{p} \cup S_\mathrm{u}$ of the external boundary be defined by

$$\begin{aligned} \mathrm{div}_2\big(k\boldsymbol{\nabla}_2\mathcal{G}\big)(\boldsymbol{x}, \boldsymbol{\xi}) + \delta(\boldsymbol{\xi} - \boldsymbol{x}) = 0 \;\; (\boldsymbol{\xi} \in \Omega), \\ \mathcal{H}(\boldsymbol{x}, \boldsymbol{\xi}) = 0 \;\; (\boldsymbol{\xi} \in S_\mathrm{p}), \\ \mathcal{G}(\boldsymbol{x}, \boldsymbol{\xi}) = 0 \;\; (\boldsymbol{\xi} \in S_\mathrm{u}), \end{aligned} \tag{27}$$

where $\mathcal{H}(\boldsymbol{x}, \boldsymbol{\xi}) = k\boldsymbol{\nabla}_2\mathcal{G}(\boldsymbol{x}, \boldsymbol{\xi})\cdot\boldsymbol{n}(\boldsymbol{\xi})$ (notations $\boldsymbol{\nabla}_\alpha$ and div_α $(\alpha = 1, 2)$ conventionally indicating the gradient and divergence w.r.t. the coordinates of the α-th argument of a two-point function). On using $w = \mathcal{G}(\boldsymbol{x}, \cdot)$, i.e. $b = \delta(\cdot - \boldsymbol{x})$, and $u_D = u_a$ (which solves the forward problem (2)–(3) with $D = D_a$) in the reciprocity identity (5), inserting boundary conditions (3), and noting that $[\![u_a]\!] = [\![v_a]\!] = \phi_a$ (because u is continuous across D_a), one obtains the following integral representation of u_a away from D_a:

$$u_a(\boldsymbol{x}) = u(\boldsymbol{x}) + \int_{D_a} \mathcal{H}(\boldsymbol{x}, \boldsymbol{\xi})\phi_a(\boldsymbol{\xi})\, \mathrm{d}s(\boldsymbol{\xi}) \qquad (\boldsymbol{x} \in \Omega_a), \tag{28}$$

where $\mathcal{H}$ is defined on D_a in terms of unit normal $\boldsymbol{n} = \boldsymbol{n}^-$ and u, the free field defined by (4), is explicitly given by

$$u(\boldsymbol{x}) = \int_{S_\mathrm{p}} \mathcal{G}(\boldsymbol{x}, \boldsymbol{\xi})\; p^\mathrm{d}(\boldsymbol{\xi})\; \mathrm{d}s(\boldsymbol{\xi}) - \int_{S_\mathrm{u}} \mathcal{H}(\boldsymbol{x}, \boldsymbol{\xi})\; u^\mathrm{d}(\boldsymbol{\xi})\; \mathrm{d}s(\boldsymbol{\xi}) \qquad (\boldsymbol{x} \in \Omega). \tag{29}$$

Similarly, the adjoint field defined by (17) admits the explicit integral representation formula

$$\hat{u}(\boldsymbol{x}) = \int_{S_\mathrm{p}} \mathcal{G}(\boldsymbol{x}, \boldsymbol{\xi})\; \varphi'_\mathrm{p}(\boldsymbol{\xi})\; \mathrm{d}s(\boldsymbol{\xi}) + \int_{S_\mathrm{u}} \mathcal{H}(\boldsymbol{x}, \boldsymbol{\xi})\; \varphi'_\mathrm{u}(\boldsymbol{\xi})\; \mathrm{d}s(\boldsymbol{\xi}) \qquad (\boldsymbol{x} \in \Omega). \tag{30}$$

A governing integral equation for ϕ_a is formulated on the basis of an integral representation for the flux associated with u_a which, for an observation point $\boldsymbol{y} \in \Omega_a$, is easily found from (28) to read

$$k\boldsymbol{\nabla}u_a(\boldsymbol{y})\cdot\boldsymbol{n}(\boldsymbol{y}) = k\boldsymbol{\nabla}u(\boldsymbol{y})\cdot\boldsymbol{n}(\boldsymbol{y}) + \int_{D_a} \mathcal{M}(\boldsymbol{y}, \boldsymbol{\xi})\phi_a(\boldsymbol{\xi})\, \mathrm{d}s(\boldsymbol{\xi}), \tag{31}$$

where $\boldsymbol{n}(\boldsymbol{y})$ is an arbitrary unit vector attached to $\boldsymbol{y}$ and $\mathcal{M}(\boldsymbol{y},\boldsymbol{\xi}) = k^2\boldsymbol{n}(\boldsymbol{y})\cdot\boldsymbol{\nabla}_{12}\mathcal{G}(\boldsymbol{y},\boldsymbol{\xi})\cdot\boldsymbol{n}(\boldsymbol{\xi})$. The integral equation then results from deriving the limiting form of (31) as $\boldsymbol{y}\to\boldsymbol{x}\in D_a$ and with $\boldsymbol{n}(\boldsymbol{y})=\boldsymbol{n}(\boldsymbol{x})$ and enforcing the boundary condition (3c) therein. This, and the ensuing asymptotic analysis, is facilitated by splitting the Green's function according to

$$\mathcal{G}(\boldsymbol{x},\boldsymbol{\xi}) = G(\boldsymbol{\xi}-\boldsymbol{x}) + G_{\mathrm{C}}(\boldsymbol{x},\boldsymbol{\xi}), \tag{32}$$

where G is the well-known (singular) fundamental solution for the 2-D full space, given by

$$G(\boldsymbol{r}) = -\frac{1}{2k\pi}\mathrm{Log}r, \qquad \boldsymbol{\nabla}G(\boldsymbol{r}) = -\frac{1}{2k\pi r^2}\boldsymbol{r} \tag{33}$$

with $r=\|\boldsymbol{r}\|$, and the complementary part G_{C} is smooth at $\boldsymbol{\xi}=\boldsymbol{x}$. On introducing spitting (32) in (31), noting the following identity (established using integration by parts, see e.g. [7])

$$\int_{D_a} M(\boldsymbol{y},\boldsymbol{\xi})\phi_a(\boldsymbol{\xi})\,\mathrm{d}s(\boldsymbol{\xi}) = -k^2\boldsymbol{\tau}(\boldsymbol{x})\cdot\int_{D_a}\boldsymbol{\nabla}_2 G(\boldsymbol{\xi}-\boldsymbol{y})\,\partial_\tau\phi_a(\boldsymbol{\xi})\,\mathrm{d}s(\boldsymbol{\xi})$$

(where $\boldsymbol{\tau}(\boldsymbol{\xi})=\boldsymbol{n}(\boldsymbol{\xi})\times\boldsymbol{e}_3$ is the unit tangent at $\boldsymbol{\xi}\in D_a$, $\partial_\tau=\boldsymbol{\tau}\cdot\boldsymbol{\nabla}$ denotes the tangential derivative, and $M(\boldsymbol{y},\boldsymbol{\xi}) = -k^2\boldsymbol{n}(\boldsymbol{y})\cdot\boldsymbol{\nabla}G(\boldsymbol{\xi}-\boldsymbol{y})\cdot\boldsymbol{n}(\boldsymbol{\xi})$), taking the limit to the boundary $\boldsymbol{y}\to\boldsymbol{x}\in D_a$ with the help of classical properties of double-layer potentials, and setting $p[u_a]$ to zero on D_a, one finally obtains the governing integral equation (wherein $M_{\mathrm{C}}(\boldsymbol{x},\boldsymbol{\xi}) = \mathcal{M}(\boldsymbol{x},\boldsymbol{\xi}) - M(\boldsymbol{x},\boldsymbol{\xi}) = k^2\boldsymbol{n}(\boldsymbol{x})\cdot\boldsymbol{\nabla}_{12}G_{\mathrm{C}}(\boldsymbol{x},\boldsymbol{\xi})\boldsymbol{n}(\boldsymbol{\xi})$):

$$k^2\boldsymbol{\tau}(\boldsymbol{x})\cdot\int_{D_a}\boldsymbol{\nabla}G(\boldsymbol{\xi}-\boldsymbol{x})\,\partial_\tau\phi_a(\boldsymbol{\xi})\,\mathrm{d}s(\boldsymbol{\xi}) - \int_{D_a} M_{\mathrm{C}}(\boldsymbol{x},\boldsymbol{\xi})\phi_a(\boldsymbol{\xi})\,\mathrm{d}s(\boldsymbol{\xi}) - p[u](\boldsymbol{x}) = 0 \quad (\boldsymbol{x}\in D_a). \tag{34}$$

4.2 Small-crack expansion of the integral equation

To study the asymptotic behaviour of integral equation (34) as $a\to 0$, it is useful to introduce other scaled geometric quantities in addition to definition (24) of $\bar{\boldsymbol{\xi}}$:

$$\boldsymbol{x} = \boldsymbol{z} + a\bar{\boldsymbol{x}}\ , \quad \boldsymbol{r} = a\bar{\boldsymbol{r}}\ , \quad r = a\bar{r} \qquad (\boldsymbol{x},\boldsymbol{\xi}\in D_a;\ \bar{\boldsymbol{x}},\bar{\boldsymbol{\xi}}\in\mathcal{D}). \tag{35}$$

Lemma 3. *Using the ansatz (26) for ϕ_a on D_a (with functions V_1, V_2, V_3 to be determined later), integral equation (34) has the following $O(a^3)$ expansion about $a=0$:*

$$\Big\{\big[\bar{\mathcal{L}}V_1\big](\bar{\boldsymbol{x}}) - \mathcal{F}_1(\bar{\boldsymbol{x}})\Big\} + a\Big\{\big[\bar{\mathcal{L}}V_2\big](\bar{\boldsymbol{x}}) - \mathcal{F}_2(\bar{\boldsymbol{x}})\Big\} + \frac{a^2}{2}\Big\{\big[\bar{\mathcal{L}}V_3\big](\bar{\boldsymbol{x}}) - \mathcal{F}_3(\bar{\boldsymbol{x}})\Big\} + o(a^2) = 0, \tag{36}$$

where the integral operator $\bar{\mathcal{L}}$ is defined for scalar, vector or tensor functions $f(\bar{\boldsymbol{\xi}})$, $\bar{\boldsymbol{\xi}}\in\mathcal{D}$ by

$$\big[\bar{\mathcal{L}}f\big](\bar{\boldsymbol{x}}) = k\boldsymbol{\tau}(\bar{\boldsymbol{x}})\cdot\int_{\mathcal{D}}\boldsymbol{\nabla}G(\bar{\boldsymbol{\xi}}-\bar{\boldsymbol{x}})\,\partial_{\bar\tau}f(\bar{\boldsymbol{\xi}})\,ds(\bar{\boldsymbol{\xi}}) \qquad (\bar{\boldsymbol{x}}\in\mathcal{D}), \tag{37}$$

(with $\partial_{\bar\tau}=\boldsymbol{\tau}(\bar{\boldsymbol{\xi}})\cdot\boldsymbol{\nabla}$ denoting the tangential derivative defined in terms of normalized coordinates $\bar{\boldsymbol{\xi}}$) and $\mathcal{F}_1(\bar{\boldsymbol{x}})$, $\mathcal{F}_2(\bar{\boldsymbol{x}})$, $\mathcal{F}_3(\bar{\boldsymbol{x}})$ are given by

$$\mathcal{F}_1(\bar{\boldsymbol{x}}) = \boldsymbol{n}(\bar{\boldsymbol{x}})\cdot\boldsymbol{\nabla}u(\boldsymbol{z}), \tag{38a}$$

$$\mathcal{F}_2(\bar{\boldsymbol{x}}) = (\boldsymbol{n}(\bar{\boldsymbol{x}})\otimes\bar{\boldsymbol{x}}):\boldsymbol{\nabla}^2u(\boldsymbol{z}), \tag{38b}$$

$$\mathcal{F}_3(\bar{\boldsymbol{x}}) = (\boldsymbol{n}(\bar{\boldsymbol{x}})\otimes\bar{\boldsymbol{x}}\otimes\bar{\boldsymbol{x}})\vdots\boldsymbol{\nabla}^3u(\boldsymbol{z}) + \boldsymbol{n}(\bar{\boldsymbol{x}})\cdot\boldsymbol{F}(\boldsymbol{z}) \tag{38c}$$

(where $\boldsymbol{\nabla}^k u(\boldsymbol{z})$ denotes the k-th order gradient of u evaluated at $\boldsymbol{\xi}=\boldsymbol{z}$), and having set

$$\boldsymbol{F}(\boldsymbol{z}) = 2k\boldsymbol{\nabla}_{12}G_C(\boldsymbol{z},\boldsymbol{z})\cdot\int_{\mathcal{D}}\boldsymbol{n}(\bar{\boldsymbol{\xi}})V_1(\bar{\boldsymbol{\xi}})\,ds(\bar{\boldsymbol{\xi}}) \tag{39}$$

In (38a–c), the symbols $:$ and $\vdots$ respectively denote inner products over two or three indices, e.g. $(\boldsymbol{n}\otimes\bar{\boldsymbol{x}}):\boldsymbol{\nabla}^2u = n_i\bar{x}_j u_{,ij}$ or $(\boldsymbol{n}\otimes\bar{\boldsymbol{x}}\otimes\bar{\boldsymbol{x}})\vdots\boldsymbol{\nabla}^3u = n_i\bar{x}_j\bar{x}_k u_{,ijk}$, with summation implied over all repeated indices (Einstein convention).

Proof. First, upon scaling the position vector according to (35) the singular full-space fundamental solution verifies

$$\boldsymbol{\nabla} G(\boldsymbol{r}) = -\frac{1}{a}\frac{1}{2k\pi\bar{r}^2}\bar{\boldsymbol{r}} = \frac{1}{a}\boldsymbol{\nabla} G(\bar{\boldsymbol{r}}), \tag{40}$$

while one has

$$\begin{aligned}\partial_\tau \phi_a(\boldsymbol{\xi}) &= \boldsymbol{\tau}(\bar{\boldsymbol{\xi}})\cdot\boldsymbol{\nabla}_\xi\Big[aV_1 + a^2V_2 + \frac{a^3}{2}V_3\Big]\big(\,(\boldsymbol{\xi}-\boldsymbol{x})/a\,\big) + o(a^3)\\ &= \partial_{\bar{\tau}}\Big[V_1 + aV_2 + \frac{a^2}{2}V_3\Big](\bar{\boldsymbol{\xi}}) + o(a^2).\end{aligned} \tag{41}$$

Using (40), (41) and arclength element scaling (25), and invoking definition (37) of $\bar{\mathcal{L}}$, one thus finds

$$k^2\boldsymbol{\tau}(\boldsymbol{x})\cdot\int_{D_a}\boldsymbol{\nabla} G(\boldsymbol{\xi}-\boldsymbol{x})\,\partial_\tau\phi_a(\boldsymbol{\xi})\,\mathrm{d}s(\boldsymbol{\xi}) = k\Big[\bar{\mathcal{L}}\Big(\,V_1 + aV_2 + \frac{a^2}{2}V_3\,\Big)\Big](\bar{\boldsymbol{x}}) + o(a^2). \tag{42}$$

Second, as the complementary kernel $M_{\mathrm{C}}(\boldsymbol{x},\boldsymbol{\xi})$ is smooth when $\boldsymbol{x}=\boldsymbol{\xi}$, one has

$$M_{\mathrm{C}}(\boldsymbol{x},\boldsymbol{\xi})\phi_a(\boldsymbol{\xi}) = k^2 a\,\big[\boldsymbol{n}(\bar{\boldsymbol{x}})\cdot\boldsymbol{\nabla}_{12}G_{\mathrm{C}}(\boldsymbol{z},\boldsymbol{z})\cdot\boldsymbol{n}(\bar{\boldsymbol{\xi}})\big]\,V_1(\bar{\boldsymbol{\xi}}) + o(a),$$

which, by virtue of scaling (25), immediately implies

$$\int_{D_a} M_{\mathrm{C}}(\boldsymbol{x},\boldsymbol{\xi})\phi_a(\boldsymbol{\xi})\,\mathrm{d}s(\boldsymbol{\xi}) = k^2a^2\boldsymbol{n}(\bar{\boldsymbol{x}})\cdot\boldsymbol{\nabla}_{12}G_{\mathrm{C}}(\boldsymbol{z},\boldsymbol{z})\cdot\int_{\mathcal{D}}\boldsymbol{n}(\bar{\boldsymbol{\xi}})V_1(\bar{\boldsymbol{\xi}})\,\mathrm{d}s(\bar{\boldsymbol{\xi}}) + o(a^2). \tag{43}$$

Third, one has the Taylor expansion

$$p[u](\boldsymbol{x}) = k\boldsymbol{n}(\bar{\boldsymbol{x}})\cdot\big[\,\boldsymbol{\nabla}u(\boldsymbol{z}) + a\boldsymbol{\nabla}^2u(\boldsymbol{z})\cdot\bar{\boldsymbol{x}} + \frac{a^2}{2}\boldsymbol{\nabla}^3u(\boldsymbol{z}):(\bar{\boldsymbol{x}}\otimes\bar{\boldsymbol{x}})\,\big] + o(a^2). \tag{44}$$

Lemma 3 then follows from substituting expansions (42), (43) and (44) into integral equation (34), reordering contributions according to powers of a and dividing the resulting equality by k. □

In the next step, the expansion of ϕ_a on D_a is found by direct application of lemma 3:

Lemma 4. *The $O(a^3)$ expansion (26) of ϕ_a on D_a is given by*

$$V_1(\bar{\boldsymbol{\xi}}) = \boldsymbol{\mathcal{U}}_1(\bar{\boldsymbol{\xi}})\cdot\boldsymbol{\nabla}u(\boldsymbol{z}), \tag{45a}$$

$$V_2(\bar{\boldsymbol{\xi}}) = \boldsymbol{\mathcal{U}}_2(\bar{\boldsymbol{\xi}}):\boldsymbol{\nabla}^2u(\boldsymbol{z}), \tag{45b}$$

$$V_3(\bar{\boldsymbol{\xi}}) = \boldsymbol{\mathcal{U}}_3(\bar{\boldsymbol{\xi}})\vdots\boldsymbol{\nabla}^3u(\boldsymbol{z}) + \boldsymbol{\mathcal{U}}_1(\bar{\boldsymbol{\xi}})\cdot\boldsymbol{F}(\boldsymbol{z}), \tag{45c}$$

where the vector function $\boldsymbol{\mathcal{U}}_1$, the second-order tensor function $\boldsymbol{\mathcal{U}}_2$ and the third-order tensor function $\boldsymbol{\mathcal{U}}_3$ do not depend on $\boldsymbol{z}$ and solve the integral equations

$$\big[\bar{\mathcal{L}}\boldsymbol{\mathcal{U}}_1\big](\bar{\boldsymbol{x}}) = \boldsymbol{n}(\bar{\boldsymbol{x}}), \tag{46a}$$

$$\big[\bar{\mathcal{L}}\boldsymbol{\mathcal{U}}_2\big](\bar{\boldsymbol{x}}) = \boldsymbol{n}(\bar{\boldsymbol{x}})\otimes\bar{\boldsymbol{x}}, \tag{46b}$$

$$\big[\bar{\mathcal{L}}\boldsymbol{\mathcal{U}}_3\big](\bar{\boldsymbol{x}}) = \boldsymbol{n}(\bar{\boldsymbol{x}})\otimes\bar{\boldsymbol{x}}\otimes\bar{\boldsymbol{x}} \tag{46c}$$

(with $\bar{\mathcal{L}}$ defined by 37). Moreover, the vector function $\boldsymbol{F}(\boldsymbol{z})$ defined by (39) is given by

$$F(\boldsymbol{z}) = 2\boldsymbol{\nabla}_{12}G_C(\boldsymbol{z},\boldsymbol{z})\cdot\boldsymbol{\mathcal{A}}_{11}\cdot\boldsymbol{\nabla}u(\boldsymbol{z}), \tag{47}$$

with the constant second-order tensor $\boldsymbol{\mathcal{A}}_{11}$ defined by

$$\boldsymbol{\mathcal{A}}_{11} = k\int_{\mathcal{D}}\boldsymbol{n}(\bar{\boldsymbol{\xi}})\otimes\boldsymbol{\mathcal{U}}_1(\bar{\boldsymbol{\xi}})\,ds(\bar{\boldsymbol{\xi}}). \tag{48}$$

Proof. The expansion (36) of integral equation (34) immediately implies that V_1, V_2, V_3 solve

$$[\bar{\mathcal{L}}V_i](\bar{\boldsymbol{x}}) = \mathcal{F}_i(\bar{\boldsymbol{x}}) \qquad (\bar{\boldsymbol{x}}\in\mathcal{D},\ i=1,2,3)$$

Representations (45a) and (45b) then readily follow from definitions (46a),(46b) and the linearity of the right-hand sides (38a) and (38b) w.r.t. $\boldsymbol{\nabla}u(\boldsymbol{z})$ and $\boldsymbol{\nabla}^2u(\boldsymbol{z})$, respectively. Similarly, since $\boldsymbol{F}(\boldsymbol{z})$ does not depend on $\bar{\boldsymbol{x}}$, one has $\bar{\mathcal{L}}(\boldsymbol{\mathcal{U}}_1(\bar{\boldsymbol{\xi}})\cdot\boldsymbol{F}(\boldsymbol{z}))](\bar{\boldsymbol{x}}) = \boldsymbol{n}(\bar{\boldsymbol{x}})\cdot\boldsymbol{F}(\boldsymbol{z})$. Representation (45c) then results from this observation together with superposition and linearity arguments. Finally, (47) and (48) follow readily from substituting representation (45a) into (39). □

Remark 4.1. From (40) and definition (33), the kernel $k\boldsymbol{\nabla}_2 G_{\mathrm{C}}(\bar{\boldsymbol{x}},\bar{\boldsymbol{\xi}})$ is dimensionless (i.e. has no physical units), and so are the normalized crack $\mathcal{D}$ and coordinates $\bar{\boldsymbol{x}},\bar{\boldsymbol{\xi}}$. This in turn makes the integral operator $\bar{\mathcal{L}}$ defined by (37) and the right-hand sides (46a–c) also dimensionless. As a result, the functions $\boldsymbol{\mathcal{U}}_1,\boldsymbol{\mathcal{U}}_2,\boldsymbol{\mathcal{U}}_3$ defined by lemma 4 are dimensionless.

Lemma 5. *Tensor functions $\boldsymbol{\mathcal{U}}_1,\boldsymbol{\mathcal{U}}_2,\boldsymbol{\mathcal{U}}_3$ defined by lemma 4 are such that*

$$\boldsymbol{\nabla}^2 w(\boldsymbol{z}) : \Big(\int_{\mathcal{D}} \boldsymbol{n}\otimes\bar{\boldsymbol{\xi}}\otimes\boldsymbol{\mathcal{U}}_1\, ds(\bar{\boldsymbol{\xi}})\Big)\cdot\boldsymbol{\nabla}\hat{w}(\boldsymbol{z}) = \boldsymbol{\nabla}\hat{w}(\boldsymbol{z})\cdot\Big(\int_{\mathcal{D}} \boldsymbol{n}\otimes\boldsymbol{\mathcal{U}}_2\, ds(\bar{\boldsymbol{\xi}})\Big) : \boldsymbol{\nabla}^2 w(\boldsymbol{z}), \quad (49a)$$

$$\boldsymbol{\nabla}^3 w(\boldsymbol{z}) \vdots \Big(\int_{\mathcal{D}} \boldsymbol{n}\otimes\bar{\boldsymbol{\xi}}\otimes\bar{\boldsymbol{\xi}}\otimes\boldsymbol{\mathcal{U}}_1\, ds(\bar{\boldsymbol{\xi}})\Big)\cdot\boldsymbol{\nabla}\hat{w}(\boldsymbol{z}) = \boldsymbol{\nabla}\hat{w}(\boldsymbol{z})\cdot\Big(\int_{\mathcal{D}} \boldsymbol{n}\otimes\boldsymbol{\mathcal{U}}_3\, ds(\bar{\boldsymbol{\xi}})\Big) \vdots \boldsymbol{\nabla}^3 w(\boldsymbol{z}) \quad (49b)$$

for any (sufficiently regular) functions $w,\hat{w}$.

Proof. Tensor functions $\boldsymbol{\mathcal{U}}_1(\bar{\boldsymbol{\xi}})\cdot\boldsymbol{\nabla}\hat{w}(\boldsymbol{z})$ and $\boldsymbol{\mathcal{U}}_2(\bar{\boldsymbol{\xi}}):\boldsymbol{\nabla}^2 w(\boldsymbol{z})$ verify the weak formulation (B.3) with $q^{\mathrm{d}}(\bar{\boldsymbol{\xi}}) = \boldsymbol{n}(\bar{\boldsymbol{\xi}})\cdot\boldsymbol{\nabla}\hat{w}(\boldsymbol{z})$ and $q^{\mathrm{d}}(\bar{\boldsymbol{\xi}}) = (\boldsymbol{n}(\bar{\boldsymbol{\xi}})\otimes\bar{\boldsymbol{\xi}}):\boldsymbol{\nabla}^2 w(\boldsymbol{z})$, respectively. On successively setting

(i) $U(\bar{\boldsymbol{\xi}}) = \boldsymbol{\mathcal{U}}_1(\bar{\boldsymbol{\xi}})\cdot\boldsymbol{\nabla}\hat{w}(\boldsymbol{z})$, $q^{\mathrm{d}}(\bar{\boldsymbol{\xi}}) = \boldsymbol{n}(\bar{\boldsymbol{\xi}})\cdot\boldsymbol{\nabla}\hat{w}(\boldsymbol{z})$, $W(\bar{\boldsymbol{\xi}}) = \boldsymbol{\mathcal{U}}_2(\bar{\boldsymbol{\xi}}):\boldsymbol{\nabla}^2 w(\boldsymbol{z})$,

(ii) $U(\bar{\boldsymbol{\xi}}) = \boldsymbol{\mathcal{U}}_2(\bar{\boldsymbol{\xi}}):\boldsymbol{\nabla}^2 w(\boldsymbol{z})$, $q^{\mathrm{d}}(\bar{\boldsymbol{\xi}}) = (\boldsymbol{n}(\bar{\boldsymbol{\xi}})\otimes\bar{\boldsymbol{\xi}}):\boldsymbol{\nabla}^2 w(\boldsymbol{z})$, $W(\bar{\boldsymbol{\xi}}) = \boldsymbol{\mathcal{U}}_1(\bar{\boldsymbol{\xi}})\cdot\boldsymbol{\nabla}\hat{w}(\boldsymbol{z})$

in (B.3) and subtracting the resulting identities (taking advantage of the obvious symmetry in (U,W) of the left-hand side of (B.3), one readily obtains identity (49a). A similar argument with $\boldsymbol{\mathcal{U}}_2(\bar{\boldsymbol{\xi}}):\boldsymbol{\nabla}^2 w(\boldsymbol{z})$ replaced with $\boldsymbol{\mathcal{U}}_3(\bar{\boldsymbol{\xi}})\vdots\boldsymbol{\nabla}^3 w(\boldsymbol{z})$ yields the other desired identity (49b). □

5 TOPOLOGICAL EXPANSION OF MISFIT FUNCTIONAL

Gathering and building upon the results of Secs. 3 and 4, the $O(a^4)$ expansion of $J(a)$ is now formulated. First, the expansion for a small crack of arbitrary shape is given in Sec. 5.1; this constitutes the main theoretical result of this article. Then, this result is specialized to the sub-class of centrally-symmetric cracks (Sec. 5.2), which includes the important special case of straight cracks (Sec. 5.3) for which further analytical treatment permit significant simplifications.

5.1 Small crack of arbitrary shape

Proposition 1. *For a crack represented by (24), i.e. of shape $\mathcal{D}$ and characteristic size a, embedded in the reference medium Ω at a chosen location $\boldsymbol{z}$, the $O(a^4)$ expansion of any objective function $J(a)$ of format (7) with densities $\varphi_p(w,\boldsymbol{\xi})$ and $\varphi_u(w,\boldsymbol{\xi})$ twice differentiable w.r.t. their first argument is*

$$J(a;\boldsymbol{z}) = J_4(a;\boldsymbol{z}) + o(a^4) \quad (50)$$

in terms of the fourth-order polynomial approximation

$$J_4(a;\boldsymbol{z}) = J(0) + \mathcal{T}_2(\boldsymbol{z})a^2 + \mathcal{T}_3(\boldsymbol{z})a^3 + \mathcal{T}_4(\boldsymbol{z})a^4, \quad (51)$$

with the coefficients $\mathcal{T}_2(\boldsymbol{z})$, $\mathcal{T}_3(\boldsymbol{z})$ and $\mathcal{T}_4(\boldsymbol{z})$ given by

$$\mathcal{T}_2(\boldsymbol{z}) = \boldsymbol{\nabla}\hat{u}(\boldsymbol{z})\cdot\boldsymbol{\mathcal{A}}_{11}\cdot\boldsymbol{\nabla}u(\boldsymbol{z}), \quad (52a)$$

$$\mathcal{T}_3(\boldsymbol{z}) = \boldsymbol{\nabla}^2 u(\boldsymbol{z}):\boldsymbol{\mathcal{A}}_{21}\cdot\boldsymbol{\nabla}\hat{u}(\boldsymbol{z}) + \boldsymbol{\nabla}^2\hat{u}(\boldsymbol{z}):\boldsymbol{\mathcal{A}}_{21}\cdot\boldsymbol{\nabla}u(\boldsymbol{z}), \quad (52b)$$

$$\begin{aligned}\mathcal{T}_4(\boldsymbol{z}) = {}& \frac{1}{2}\boldsymbol{\nabla}^3 u(\boldsymbol{z})\vdots\boldsymbol{\mathcal{A}}_{31}\cdot\boldsymbol{\nabla}\hat{u}(\boldsymbol{z}) + \frac{1}{2}\boldsymbol{\nabla}^3\hat{u}(\boldsymbol{z})\vdots\boldsymbol{\mathcal{A}}_{31}\cdot\boldsymbol{\nabla}u(\boldsymbol{z}) + \boldsymbol{\nabla}^2\hat{u}(\boldsymbol{z}):\boldsymbol{\mathcal{A}}_{22}:\boldsymbol{\nabla}^2 u(\boldsymbol{z}) \\ & + \boldsymbol{\nabla}\hat{u}(\boldsymbol{z})\cdot\boldsymbol{\mathcal{B}}_{11}\cdot\boldsymbol{\nabla}u(\boldsymbol{z}) + \frac{1}{2}\int_{S_p}\varphi_p'' W^2\, ds + \frac{1}{2}\int_{S_u}\varphi_u'' Q^2\, ds. \end{aligned} \quad (52c)$$

In (52a–c), the function W is given by

$$W(\boldsymbol{x}) = \boldsymbol{\nabla}_2\mathcal{G}(\boldsymbol{x},\boldsymbol{z})\cdot\boldsymbol{\mathcal{A}}_{11}\cdot\boldsymbol{\nabla}u(\boldsymbol{z}) \quad (53)$$

and $Q = k\boldsymbol{\nabla} W\cdot\boldsymbol{n}$, the constant tensors $\boldsymbol{\mathcal{A}}_{11}, \boldsymbol{\mathcal{A}}_{12}, \boldsymbol{\mathcal{A}}_{13}, \boldsymbol{\mathcal{A}}_{22}$ are given by (48) and

$$\boldsymbol{\mathcal{A}}_{21} = k\int_{\mathcal{D}} \boldsymbol{n}\otimes\bar{\boldsymbol{\xi}}\otimes\boldsymbol{\mathcal{U}}_1\, ds(\bar{\boldsymbol{\xi}}), \tag{54a}$$

$$\boldsymbol{\mathcal{A}}_{31} = k\int_{\mathcal{D}} \boldsymbol{n}\otimes\bar{\boldsymbol{\xi}}\otimes\bar{\boldsymbol{\xi}}\otimes\boldsymbol{\mathcal{U}}_1\, ds(\bar{\boldsymbol{\xi}}), \tag{54b}$$

$$\boldsymbol{\mathcal{A}}_{22} = k\int_{\mathcal{D}} \boldsymbol{n}\otimes\bar{\boldsymbol{\xi}}\otimes\boldsymbol{\mathcal{U}}_2\, ds(\bar{\boldsymbol{\xi}}) \tag{54c}$$

in terms of solutions $\boldsymbol{\mathcal{U}}_1, \boldsymbol{\mathcal{U}}_2$ to equations (46a,b), and the constant tensor $\boldsymbol{\mathcal{B}}_{11}$ is given by

$$\boldsymbol{\mathcal{B}}_{11} = \boldsymbol{\mathcal{A}}_{11}\cdot\boldsymbol{\nabla}_{12}G_C(\boldsymbol{z},\boldsymbol{z})\cdot\boldsymbol{\mathcal{A}}_{11}. \tag{55}$$

Proof. The proof is straightforward, and consists in deriving an explicit form for expansion (18). In particular, the expansion of the first integral of (18) exploits the results of Sec. 4.

(a) First integral of (18). Invoking expansion (26) of ϕ_a, representation formulae (45a–c) for V_1, V_2, V_3, normalized coordinates (24), and Taylor expansion

$$p[\hat{u}](\boldsymbol{\xi}) = k\boldsymbol{n}(\bar{\boldsymbol{\xi}})\cdot\Big\{\boldsymbol{\nabla}\hat{u}(\boldsymbol{z}) + a\boldsymbol{\nabla}^2\hat{u}(\boldsymbol{z})\cdot\bar{\boldsymbol{\xi}} + \frac{a^2}{2}\boldsymbol{\nabla}^3\hat{u}(\boldsymbol{z}):(\bar{\boldsymbol{\xi}}\otimes\bar{\boldsymbol{\xi}})\Big\} + o(a^2) \qquad (\boldsymbol{\xi}\in D_a,\ \bar{\boldsymbol{\xi}}\in\mathcal{D})$$

for the adjoint field, one readily obtains

$$\begin{aligned}
[p[\hat{u}]\phi_a](\boldsymbol{\xi}) = {}& ka\boldsymbol{\nabla}\hat{u}(\boldsymbol{z})\cdot(\boldsymbol{n}(\bar{\boldsymbol{\xi}})\otimes\boldsymbol{\mathcal{U}}_1(\bar{\boldsymbol{\xi}}))\cdot\boldsymbol{\nabla}u(\boldsymbol{z})\\
&+ ka^2\Big\{\boldsymbol{\nabla}\hat{u}(\boldsymbol{z})\cdot(\boldsymbol{n}(\bar{\boldsymbol{\xi}})\otimes\boldsymbol{\mathcal{U}}_2(\bar{\boldsymbol{\xi}})):\boldsymbol{\nabla}^2u(\boldsymbol{z}) + \boldsymbol{\nabla}^2\hat{u}(\boldsymbol{z}):(\boldsymbol{n}(\bar{\boldsymbol{\xi}})\otimes\bar{\boldsymbol{\xi}}\otimes\boldsymbol{\mathcal{U}}_1(\bar{\boldsymbol{\xi}}))\cdot\boldsymbol{\nabla}u(\boldsymbol{z})\Big\}\\
&+ k\frac{a^3}{2}\Big\{\boldsymbol{\nabla}\hat{u}(\boldsymbol{z})\cdot(\boldsymbol{n}(\bar{\boldsymbol{\xi}})\otimes\boldsymbol{\mathcal{U}}_3(\bar{\boldsymbol{\xi}})):\boldsymbol{\nabla}^3u(\boldsymbol{z}) + 2\boldsymbol{\nabla}^2\hat{u}(\boldsymbol{z}):(\boldsymbol{n}(\bar{\boldsymbol{\xi}})\otimes\bar{\boldsymbol{\xi}}\otimes\boldsymbol{\mathcal{U}}_2(\bar{\boldsymbol{\xi}})):\boldsymbol{\nabla}^2u(\boldsymbol{z})\\
&\quad + \boldsymbol{\nabla}^3\hat{u}(\boldsymbol{z})\vdots(\boldsymbol{n}(\bar{\boldsymbol{\xi}})\otimes\bar{\boldsymbol{\xi}}\otimes\bar{\boldsymbol{\xi}}\otimes\boldsymbol{\mathcal{U}}_1(\bar{\boldsymbol{\xi}}))\cdot\boldsymbol{\nabla}u(\boldsymbol{z}) + \big(\boldsymbol{\nabla}\hat{u}(\boldsymbol{z})\cdot\boldsymbol{n}(\bar{\boldsymbol{\xi}})\big)\,\big(\boldsymbol{\mathcal{U}}_1(\bar{\boldsymbol{\xi}})\cdot\boldsymbol{F}(\boldsymbol{z})\big)\Big\}\\
&+ o(a^3) \qquad (\boldsymbol{\xi}\in D_a,\ \bar{\boldsymbol{\xi}}\in\mathcal{D}).
\end{aligned} \tag{56}$$

Integrating this expansion over D_a (using scaled coordinates), exploiting identities (49a), (49b) and recalling definitions (48), (54a,c) and (55) of the various constant tensors, one obtains

$$\begin{aligned}
\int_{D_a} p[\hat{u}](\boldsymbol{\xi})\phi_a(\boldsymbol{\xi})\,\mathrm{d}s(\bar{\boldsymbol{\xi}}) = {}& a^2\boldsymbol{\nabla}\hat{u}(\boldsymbol{z})\cdot\boldsymbol{\mathcal{A}}_{11}\cdot\boldsymbol{\nabla}u(\boldsymbol{z})\\
&+ a^3\Big\{\boldsymbol{\nabla}^2\hat{u}(\boldsymbol{z}):\boldsymbol{\mathcal{A}}_{21}\cdot\boldsymbol{\nabla}u(\boldsymbol{z}) + \boldsymbol{\nabla}^2u(\boldsymbol{z}):\boldsymbol{\mathcal{A}}_{21}\cdot\boldsymbol{\nabla}\hat{u}(\boldsymbol{z})\Big\}\\
&+ a^4\Big\{\frac{1}{2}\boldsymbol{\nabla}^3\hat{u}(\boldsymbol{z})\vdots\boldsymbol{\mathcal{A}}_{31}\cdot\boldsymbol{\nabla}u(\boldsymbol{z}) + \frac{1}{2}\boldsymbol{\nabla}^3u(\boldsymbol{z})\vdots\boldsymbol{\mathcal{A}}_{31}\cdot\boldsymbol{\nabla}\hat{u}(\boldsymbol{z})\\
&\quad + \boldsymbol{\nabla}^2u(\boldsymbol{z}):\boldsymbol{\mathcal{A}}_{22}:\boldsymbol{\nabla}^2\hat{u}(\boldsymbol{z}) + \boldsymbol{\nabla}\hat{u}(\boldsymbol{z})\cdot\boldsymbol{\mathcal{B}}_{11}\cdot\boldsymbol{\nabla}u(\boldsymbol{z})\Big\} + o(a^4).
\end{aligned} \tag{57}$$

(b) Second and third integrals of (18). The perturbed field v_a at any point away from the crack is given by (28), i.e.:

$$v_a(\boldsymbol{x}) = \int_{D_a}\mathcal{H}(\boldsymbol{x},\boldsymbol{\xi})\phi_a(\boldsymbol{\xi})\,\mathrm{d}s(\boldsymbol{\xi}) \qquad (\boldsymbol{x}\in\Omega\setminus D_a). \tag{58}$$

As $\mathcal{G}(\boldsymbol{x},\boldsymbol{\xi})$ is a smooth function of $\boldsymbol{\xi}\in D_a$ for any $\boldsymbol{x}\notin D_a$, the leading contribution of $v_a(\boldsymbol{x})$ as $a\to 0$ is found by setting $\phi_a(\boldsymbol{\xi}) = aV_1(\bar{\boldsymbol{\xi}}) + o(a)$ and invoking scaling (25) in (58), to obtain

$$v_a(\boldsymbol{x}) = ka^2\boldsymbol{\nabla}_2\mathcal{G}(\boldsymbol{z},\boldsymbol{z})\cdot\int_{\mathcal{D}}\boldsymbol{n}(\bar{\boldsymbol{\xi}})V_1(\bar{\boldsymbol{\xi}})\,\mathrm{d}s(\bar{\boldsymbol{\xi}}) + o(a^2) = a^2W(\boldsymbol{x};\boldsymbol{z}) + o(a^2),$$
$$\text{with}\quad W(\boldsymbol{x};\boldsymbol{z}) = \boldsymbol{\nabla}_2\mathcal{G}(\boldsymbol{z},\boldsymbol{z})\cdot\boldsymbol{\mathcal{A}}_{11}\cdot\boldsymbol{\nabla}u(\boldsymbol{z}) \tag{59}$$

(with the last equality stemming from (45a) and (48)) i.e. representation (22) and result (53). Then, plugging (59) and the corresponding value of $q_a = p[v_a]$ into the last two integrals of (18) yields the two integral terms of (52c). This completes the proof. □

Remark 5.1. The coefficient $\mathcal{T}_2(\boldsymbol{z})$ associated with the leading $O(a^2)$ contribution to $J(a)$ is, as expected, equal to the previously known topological derivative of J, i.e. (20).

Remark 5.2. As a consequence of reciprocity identity (49b), $\boldsymbol{\mathcal{U}}_3$ does not explicitly appear in the final form of the $O(a^4)$ expansion of $J(a)$ (all the constant tensors featured in (52a-c) being expressed in terms of $\boldsymbol{\mathcal{U}}_1, \boldsymbol{\mathcal{U}}_2$ only), making the actual computation of $\boldsymbol{\mathcal{U}}_3$ unnecessary (however, reaching this result required that the governing equation for $\boldsymbol{\mathcal{U}}_3$ be established).

5.2 Centrally-symmetric crack

When D_a has central symmetry (i.e. is such that $\bar{\boldsymbol{\xi}} \in \mathcal{D} \Leftrightarrow -\bar{\boldsymbol{\xi}} \in \mathcal{D}$), the constant tensor $\boldsymbol{\mathcal{A}}_{21}$ defined by (54a) vanishes, as shown in Appendix A. Consequently:

Proposition 2. *When the crack of Proposition 1 has central symmetry, expansion (50) holds with coefficients $\mathcal{T}_2, \mathcal{T}_4$ still given by (52a,c) and*

$$\mathcal{T}_3(\boldsymbol{z}) = 0. \tag{60}$$

5.3 Straight crack

The special case of a *straight* crack D_a (where $\mathcal{D}$ is a line segment of length 2) is now considered. Of course, as the straight crack has central symmetry, simplification (60) holds, but this special case permits further analytical treatment, as integral equations (46a,c) are solvable in closed form.

Lemma 6. *Let $\mathcal{D}$ denote the normalized straight crack $\mathcal{D} = \{-1 \leq \bar{\xi}_1 \leq 1,\ \bar{\xi}_2 = 0\}$ with unit tangent $\boldsymbol{\tau} = \boldsymbol{e}_1$ and normal $\boldsymbol{n} = \boldsymbol{e}_2$. With $\bar{x}_1, \bar{\xi}_1$ simply denoted $\bar{x}, \bar{\xi}$ for simplicity, the solutions of integral equations (46a,c) are given by*

$$\boldsymbol{\mathcal{U}}_1(\bar{\boldsymbol{x}}) = 2(1-\bar{x}^2)^{1/2}\, \boldsymbol{n}, \tag{61a}$$

$$\boldsymbol{\mathcal{U}}_2(\bar{\boldsymbol{x}}) = (1-\bar{x}^2)^{1/2} \bar{x}\, \boldsymbol{n} \otimes \boldsymbol{\tau}, \tag{61b}$$

$$\boldsymbol{\mathcal{U}}_3(\bar{\boldsymbol{x}}) = \frac{1}{3}(1-\bar{x}^2)^{1/2}(2\bar{x}^2+1)\, \boldsymbol{n} \otimes \boldsymbol{\tau} \otimes \boldsymbol{\tau}. \tag{61c}$$

Proof. See Appendix B □

Explicit formulae for the constant tensors $\boldsymbol{\mathcal{A}}_{11}, \boldsymbol{\mathcal{A}}_{22}, \boldsymbol{\mathcal{A}}_{31}$ featured in (52a,c) then readily follow:

Proposition 3. *Under the assumptions of Lemma 6, the constant tensors $\boldsymbol{\mathcal{A}}_{11}, \boldsymbol{\mathcal{A}}_{22}, \boldsymbol{\mathcal{A}}_{31}$ are given by*

$$\boldsymbol{\mathcal{A}}_{11} = k\pi \boldsymbol{n} \otimes \boldsymbol{n}\,, \quad \boldsymbol{\mathcal{A}}_{22} = \frac{k\pi}{8} \boldsymbol{n} \otimes \boldsymbol{\tau} \otimes \boldsymbol{n} \otimes \boldsymbol{\tau}\,, \quad \boldsymbol{\mathcal{A}}_{31} = \frac{k\pi}{4} \boldsymbol{n} \otimes \boldsymbol{\tau} \otimes \boldsymbol{\tau} \otimes \boldsymbol{n}. \tag{62}$$

In addition, the case of a straight crack appearing at the center of a disk is given an analytical treatment in Appendix C. Such results are useful as they illustrate the general methodology, give insight into its details and permit a check of its consistency.

5.4 Discussion

Implementation and computational efficiency issues. The foregoing developments and results are based on the Green's function $\mathcal{G}$ defined by (27). They lead to almost-explicit formulae for the $O(a^4)$ expansion of $J(a)$ (the only non-explicit components being the auxiliary solutions $\boldsymbol{\mathcal{U}}_1, \boldsymbol{\mathcal{U}}_2$, which must be computed numerically except for simple crack shapes such as the straight crack). In practice, this explicit character is retained only for a few simple geometries Ω and boundary conditions settings $S_\mathrm{p}, S_\mathrm{u}$ for which $\mathcal{G}$ is known analytically. These include the half-plane (where $\mathcal{G}$ is given by the well-known method of images) and the circular disk (see Eq. (C.1) in Appendix C).

For other configurations, the main computational tasks required for evaluating coefficients $\mathcal{T}_2(\boldsymbol{z})$ and $\mathcal{T}_4(\boldsymbol{z})$ of expansion (50,51) as functions of the sampling points $\boldsymbol{z}$ (assuming for simplicity a

centrally-symmetric, e.g. straight, small trial crack) are the following: (a) compute the free field u and its gradients up to the third order, (b) compute the adjoint field $\hat{u}$ and its gradients up to the third order, (c) compute $W(\boldsymbol{x}),\ \boldsymbol{x} \in S_{\mathrm{p}}$ and $Q(\boldsymbol{x}),\ \boldsymbol{x} \in S_{\mathrm{u}}$ (d) compute $\boldsymbol{\nabla}_{12} G_{\mathrm{C}}(\boldsymbol{z}, \boldsymbol{z})$ as a function of $\boldsymbol{z}$. All these tasks can be formulated in terms of solving standard boundary integral equations [7, 13] featuring the full-space fundamental solution, using the procedure presented in [9]. Following this approach (which is employed in the ensuing examples), tasks (a) and (b) each require one BEM solution, while tasks (c) and (d) each require one BEM solution per sampling point (with all tasks entailing subsequent integral representation evaluations). All BEM problems are formulated on the same (reference) configuration and with the same boundary condition structure. This allows to set up, store and factor the BEM influence matrix once and for all, each BEM solution then only requiring to set up one right-hand side and perform one backsubstitution. In contrast, conventional global minimization approaches are much more computation-intensive as they entail solving large numbers of forward problems on as many different configurations (thus requiring each time to set up and factor the BEM influence matrix anew). Repeated analyses on the same configuration may be further facilitated by the fact that many of the boundary-value problems of interest (e.g. all those pertaining to the Green's function) can be solved offline as a preliminary preparatory step.

Alternatively, finite element methods (FEMs) might also be used for setting up expansions of the form (50), although coefficient $\mathcal{T}_4$ entails computing second- and third-order gradients of the free and adjoint fields, which normally requires specially-designed procedures and raises accuracy issues (while integral representations of higher-order gradients do not).

Direct vs. adjoint approaches for topological sensitivity. Topological sensitivity formulas are formally similar to usual formulas for first-order parameter sensitivity [20] or shape sensitivity [27]. Like the latter, the topological derivative $\mathcal{T}_2$ is expressed as a bilinear combination of the free and adjoint fields. Moreover, setting up the highest-order coefficient $\mathcal{T}_4$ requires the 'direct topological field sensitivities' W, Q, in addition to the free and adjoint fields, which is formally similar to second-order parameter or shape sensitivities expressed as bilinear combinations of the free and adjoint fields and their first-order sensitivities. Finally, topological and shape sensitivities, while related, are distinct concepts, as emphasized in [12].

The $O(a^4)$ expansion of $J(a)$ could alternatively have been established on the basis of (13) rather than (18), without recourse to the adjoint solution (17). This 'direct' approach requires $O(a^4)$ expansions of v_a on S_{p} and q_a on S_{u}, i.e. the computation of higher-order topological field sensitivities W_2, W_3 in addition to $W = W_1$ defined in (22). General explicit formulae for such high-order expansions of field quantities are given in [2] in terms of the Green's function and its derivatives.

The case of smoothly-heterogeneous materials. A spatially-constant conductivity k has been assumed in the foregoing developments for simplicity. However, the formal analysis carries over to smoothly-heterogeneous conductivity distributions $k(\boldsymbol{\xi})$ with very few changes (in particular, the Green's function $\mathcal{G}$ can still be defined by (27), although it is usually not known in closed form even for simple geometries), using the fact that replacing the conductivity in a neighbourhood of a vanishing crack $D_a(\boldsymbol{z})$ by the constant conductivity $k(\boldsymbol{\xi}) = k(\boldsymbol{z})$ yield the correct leading behavior in the limit $a \to 0$ (see [11] for penetrable obstacles in inhomogeneous acoustic media).

6 NUMERICAL RESULTS

Numerical experiments on crack identification using the proposed $O(a^4)$ expansion of least-squares output misfit function (7) have been performed on the following configuration (Fig. 3). The reference domain Ω is the square $\Omega =]0,1[\times]0,1[$. The boundary conditions are as follows: a potential $u^{\mathrm{d}} = 0$ is imposed on $S_{\mathrm{u}}^{(1)}$ and $S_{\mathrm{u}}^{(2)}$, a constant flux p_i^{d} on $S_{\mathrm{p}}^{(i)}$, $i = 1, \ldots, 4$ (with values of p_i^{d} to be specified shortly), and the remaining part $S \backslash (S_{\mathrm{u}}^{(1)} \cup S_{\mathrm{u}}^{(2)} \cup S_{\mathrm{p}}^{(1)} \cup \ldots \cup S_{\mathrm{p}}^{(4)})$ of the boundary is insulated ($p^{\mathrm{d}} = 0$). The overdetermined boundary data used for crack identification consists of known values u^{obs} of the potential over the complete Neumann surface $S_{\mathrm{p}} = S \setminus (S_{\mathrm{u}}^{(1)} \cup S_{\mathrm{u}}^{(2)})$ induced by given excitations

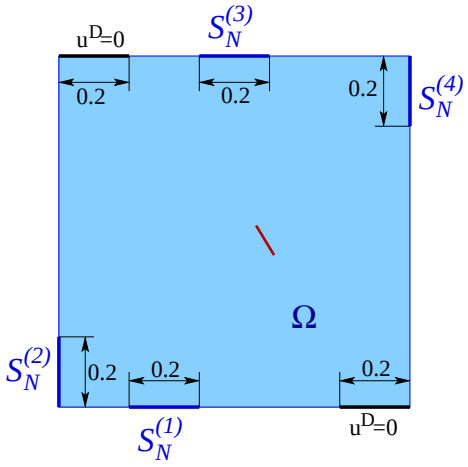

Figure 3: *Numerical examples: geometry and boundary conditions for reference configuration.*

p_i^{d}. M simulated experiments, labelled $m = 1, \ldots, M$, are considered, with data p_i^{d} for the m-th experiment defined by $p_i^{\mathrm{d}} = \delta_{im}$ (with $M = 1, 2, 4$ considered in the results to follow). The output least-squares misfit function, corresponding to φ_{p} defined by (8) and $\varphi_{\mathrm{u}} = 0$, is thus

$$\mathcal{J}_{\mathrm{LS}}(D) = \frac{1}{2} \sum_{m=1}^{M} \int_{S_{\mathrm{p}}} \left| u_{Dm}(\boldsymbol{\xi}) - u_m^{\mathrm{obs}}(\boldsymbol{\xi}) \right|^2 \mathrm{d}s. \tag{63}$$

For each simulated experiment, both the free-field u_m and the exact synthetic data u_m^{true}, corresponding respectively to the reference domain (i.e. $D = \emptyset$) and the true perturbed configurations with one crack of finite size, are computed using a standard boundary element method (BEM), with piecewise-linear and piecewise-constant interpolations, respectively, for potentials and fluxes. The data u_m^{obs} featured in (63) is then obtained by corrupting u_m^{true} by simulated noise. Cracks are represented as very elongated insulated cavities (with an aspect ratio of 40:1) for the gerenation of synthetic data, so that a slight modelling error is introduced. The Green's function $\mathcal{G}$ not being known in closed form, G_{C} is numerically evaluated via a BEM solution of the boundary value problem

$$k\Delta G_{\mathrm{C}}(\boldsymbol{x}, \cdot) = 0 \ \text{ in } \Omega\,, \quad H_{\mathrm{C}}(\boldsymbol{x}, \cdot) = -H(\boldsymbol{x}, \cdot) \ \text{ on } S_{\mathrm{p}}\,, \quad G_{\mathrm{C}}(\boldsymbol{x}, \cdot) = -G(\cdot - \boldsymbol{x}) \ \text{ on } S_{\mathrm{u}}, \tag{64}$$

Taking advantage of the fact that the relevant integral operator does not depend on $\boldsymbol{x}$, this only entails computing a right-hand side and performing a backsubstitution for each $\boldsymbol{x}$ (with $\boldsymbol{x}$ taken as each sampling point in turn), and hence defines a computationally reasonable task.

6.1 Approximate global search procedure

Following the approach previously proposed in [9] for inclusion identification, define a fine search grid $\mathbf{G}$, i.e. a (dense) discrete set of sampling points $\boldsymbol{z}$ spanning (part of) the interior of Ω. Partial minimization w.r.t. a of the fourth-degree polynomial approximation $J_4(a; \boldsymbol{z})$ of $\mathcal{J}_{\mathrm{LS}}$ for given $\boldsymbol{z} \in \mathbf{G}$ is a very simple, and light, task that can be easily performed for all $\boldsymbol{z} \in \mathbf{G}$. In this section, $J_4(a; \boldsymbol{z})$ is defined in terms of straight trial cracks, so that $\mathcal{T}_3(\boldsymbol{z}) = 0$ and the constant tensors featured in expressions (52a,c) of $\mathcal{T}_2$, $\mathcal{T}_4$ are given by (55) and (62). A partial minimizer $a = \ell(\boldsymbol{z})$ of $J_4(\cdot, \boldsymbol{z})$ must verify

$$\frac{\partial J_4}{\partial a}(\cdot; \boldsymbol{z}) = 0, \qquad \text{i.e.} \quad \ell^2(\boldsymbol{z}) = -\frac{\mathcal{T}_2(\boldsymbol{z})}{2\mathcal{T}_4(\boldsymbol{z})}. \tag{65}$$

For (65) to actually yield a real-valued non-zero partial minimizer of $J_4(\cdot, \boldsymbol{z})$ at $\boldsymbol{z}$, one must have $\mathcal{T}_2(\boldsymbol{z}) < 0$ and $\mathcal{T}_4(\boldsymbol{z}) > 0$. Next, for any $\boldsymbol{z} \in \mathbf{G}$ meeting these conditions, let

$$J^{\min}(\boldsymbol{z}) = J_4(\ell(\boldsymbol{z}); \boldsymbol{z}) = J(0) - \frac{\mathcal{T}_2^2(\boldsymbol{z})}{4\mathcal{T}_4(\boldsymbol{z})}. \tag{66}$$

		S1			S2			S3		
		$\sigma=0$	$\sigma=0.2$	$\sigma=0.4$	$\sigma=0$	$\sigma=0.2$	$\sigma=0.4$	$\sigma=0$	$\sigma=0.2$	$\sigma=0.4$
$\ell^{\text{true}}=0.04$	$\boldsymbol{x}^{\text{est}}$	0	0	4	0	0	0	0	0	0
	ℓ^{est}	0.0403	0.0396	0.0389	0.0403	0.0403	0.0405	0.0403	0.0404	0.0405
$\ell^{\text{true}}=0.06$	$\boldsymbol{x}^{\text{est}}$	0	4	1	0	0	0	0	0	0
	ℓ^{est}	0.0599	0.0594	0.0592	0.0605	0.0605	0.0607	0.0606	0.0609	0.0607
$\ell^{\text{true}}=0.08$	$\boldsymbol{x}^{\text{est}}$	0	3	5	0	0	0	0	0	0
	ℓ^{est}	0.0800	0.0796	0.0817	0.0810	0.0813	0.0820	0.0810	0.0808	0.0805
$\ell^{\text{true}}=0.10$	$\boldsymbol{x}^{\text{est}}$	2	0	0	0	0	0	0	0	0
	ℓ^{est}	0.101	0.099	0.099	0.102	0.102	0.100	0.102	0.102	0.102
$\ell^{\text{true}}=0.12$	$\boldsymbol{x}^{\text{est}}$	0	0	6	0	0	0	0	0	0
	ℓ^{est}	0.122	0.119	0.123	0.123	0.123	0.123	0.121	0.122	0.122

Table 1: *Identification of buried straight crack of half-length ℓ^{true}: estimated location $\boldsymbol{x}^{est}$ and size ℓ^{est}. Found estinated locations $\boldsymbol{x}^{est}$ are labelled as follows:* $0 \leftarrow \boldsymbol{x}^{est}=(0.6,\,0.48)$ *(closest to* $\boldsymbol{x}^{true}$*),* $1 \leftarrow \boldsymbol{x}^{est}=(0.6,\,0.5)$, $2 \leftarrow \boldsymbol{x}^{est}=(0.58,\,0.48)$, $3 \leftarrow \boldsymbol{x}^{est}=(0.62,\,0.48)$, $4 \leftarrow \boldsymbol{x}^{est}=(0.62,\,0.46)$, $5 \leftarrow \boldsymbol{x}^{est}=(0.58,\,0.5)$, $6 \leftarrow \boldsymbol{x}^{est}=(0.56,\,0.5)$.

The best estimate of the unknown crack D^{true} yielded by this procedure is then defined by the location $\boldsymbol{z}^{\text{est}}$ and size ℓ^{est} achieving the lowest value of $J_4(a;\boldsymbol{z})$ over $\mathbf{G}$, i.e. given by

$$\boldsymbol{z}^{\text{est}} = \arg\min_{\boldsymbol{z}\in\mathbf{G}} J^{\min}(\boldsymbol{z}), \qquad \ell^{\text{est}} = \ell(\boldsymbol{z}^{\text{est}}). \tag{67}$$

This approach can be viewed as an approximate global search procedure over the spatial region being sampled, which is computationally much less expensive than usual global search algorithms.

6.2 Numerical results for crack identification

This procedure is now applied to the identification, from simulated data, of a straight crack D^{true} of length $2\ell^{\text{true}}$ centered at $\boldsymbol{x}^{\text{true}}=(0.605,\,0.475)$, whose orientation is defined in terms of the angle φ^{true} entering the definition of the unit normal $\boldsymbol{n}^{\text{true}}=(\cos\varphi^{\text{true}},\sin\varphi^{\text{true}})$ to D^{true}. Five crack lengths $\ell^{\text{true}}=0.04,\,0.06,\,0.08,\,0.1,\,0.12$ are considered, with the actual crack orientation always defined by $\varphi^{\text{true}}=3\pi/5$. Synthetic data u^{obs} is computed for each true crack size ℓ^{true} and excitation p_i^{d} (using a BEM model with 400 elements on S and 400 on D^{true}). The effect of imperfect data is tested by defining u^{obs} as a perturbed version of u^{true} according to

$$u^{\text{obs}} = u^{\text{true}} + \sigma\chi\|u-u^{\text{true}}\|_{L^2(S_{\text{p}})},$$

where χ is a uniform random variable with zero mean and unit standard deviation.

A search grid $\mathbf{G}$ of 35×35 regularly spaced sampling points covering the square region $0.16\le x_1,x_2\le 0.84$ is defined (the grid spacing being hence $\Delta x_1=\Delta x_2=0.02$). All computations are implemented using Matlab and run on a laptop PC. On this platform, the complete approximate global search procedure was found to require about 2 minutes of computation time. Most of this time went into the many evaluations of integral representations needed by a BEM-based implementation, a task whose efficiency can be improved as the current, simple, Matlab coding is slowed down by loops.

Results for the identified location $\boldsymbol{z}^{\text{est}}$ and size ℓ^{est} of the unknown crack using $M=4$ experiments are presented in Table 1 for the five true crack lengths, data corruption levels defined by $\sigma=0,\,0.2,\,0.4$, and three sensor sets S1, S2 and S3 of increasing density. Set S3 assumes that the potential is known at all BE nodes of S_{p}, while measurements are available only every 20 nodes (set S1) or every 5 nodes (set S2), with the integral cost functional (63) defined using linear interpolation of u^{obs} between sensors. Disregarding nodes located on S_{u}, S1, S2 and S3 thus feature 16, 70 and 358 sensors, respectively. Estimated crack lengths ℓ^{est} are found to be within at most about 3% of ℓ^{true}, with data corruption and variations in sensor density affecting only mildly the results. Moreover, the estimated location $\boldsymbol{z}^{\text{est}}$ coincides in most cases with the grid point $\boldsymbol{z}=(0.6,\,0.48)$ which is

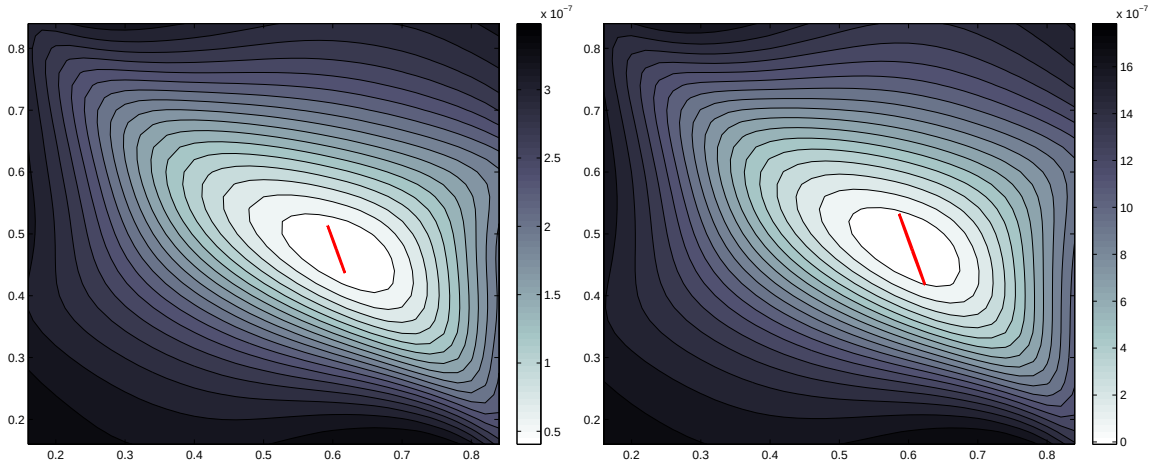

Figure 4: *Distribution of $J^{min}(\boldsymbol{z})$ over search grid $\mathbf{G}$, and outline of true crack. Left: sensor set S1, $\ell^{true} = 0.4$ and $\sigma = 0.4$. Right: sensor set S3, $\ell^{true} = 0.6$ and $\sigma = 0.$.*

closest to $\boldsymbol{z}^{\text{true}}$, with all the departures from this situation occurring for the coarsest sensor set S1 and yielding estimated locations $\boldsymbol{z}^{\text{est}}$ whose distance to $\boldsymbol{z}^{\text{true}}$ is at most $(0.045^2 + 0.025^2)^{1/2} \approx 0.051$. Additionally, the function $J^{\text{min}}(\boldsymbol{z})$, shown together with the outline of D^{true} on Fig. 4 for two of the cases reported in Table 1, is seen to attain values close to its global minimum only in the vicinity of the actual crack (a behavior which was observed for all tested configurations).

The effect of the number M of experiments is considered next. Table 2 shows results obtained for the five true crack lengths, using the densest sensor set S3 and no noise ($\sigma = 0$), using $M = 1$, 2 or 4 experiments. In two cases ($\ell^{\text{true}} = 0.1,\ 0.12$), the search procedure did not perform adequately as the conditions $\mathcal{T}_2(\boldsymbol{z}) < 0$ and $\mathcal{T}_4(\boldsymbol{z}) > 0$ required for $J_4(\cdot, \boldsymbol{z})$ to actually have a minimum were not met at several grid locations, while the results delivered by (67) were grossly incorrect at some of the remaining grid points. The other cases yielded acceptable results, only mildly affected by M. Overall, such breakdown was observed for cases with $M = 1$ (sometimes) or $M = 2$ (rarely), but never for $M = 4$. This suggests that the dominant factor for achieving robust identification is the number of experiments rather than the sensor density available for each experiment. A sample of results from Table 2 is illustrated in terms of contour plots of the function $J^{\text{min}}(\boldsymbol{z})$ in Fig. 5.

All the foregoing numerical results were obtained on the assumption that the normal to the crack is known, i.e. $\boldsymbol{n} = \boldsymbol{n}^{\text{true}}$ and $\boldsymbol{\tau} = \boldsymbol{e}_3 \times \boldsymbol{n}^{\text{true}}$ were used in expressions (62) of the constant tensors $\boldsymbol{\mathcal{A}}_{11}$, $\boldsymbol{\mathcal{A}}_{22}$, $\boldsymbol{\mathcal{A}}_{31}$. The reciprocity gap method [5] provides a means to identify the normal $\boldsymbol{n} = \boldsymbol{n}^{\text{true}}$ from complete overdetermined data on the boundary. Absent prior identification of $\boldsymbol{n} = \boldsymbol{n}^{\text{true}}$, one may treat the angle φ such that $\boldsymbol{n} = (\cos\varphi, \sin\varphi)$ as an additional unknown. In that case, $\mathcal{T}_2$, $\mathcal{T}_4$, ℓ and J^{min} are functions of $\boldsymbol{z}, \varphi$, through the φ-dependence of $\boldsymbol{\mathcal{A}}_{11}$, $\boldsymbol{\mathcal{A}}_{22}$, $\boldsymbol{\mathcal{A}}_{31}$, and the final estimation step (67) becomes

$$\big(\boldsymbol{z}^{\text{est}},\, \varphi^{\text{est}}\big) = \underset{\boldsymbol{z}\in\mathbf{G},\, 0\le\varphi<\pi}{\arg\min} \Big(J(0) - \frac{\mathcal{T}_2^2(\boldsymbol{z},\varphi)}{2\mathcal{T}_4(\boldsymbol{z},\varphi)}\Big), \qquad \ell^{\text{est}} = \ell(\boldsymbol{z}^{\text{est}}, \varphi). \tag{68}$$

# of measurements:	1	2	4
$\ell^{\text{true}} = 0.04$	0.0404	0.0403	0.0404
$\ell^{\text{true}} = 0.06$	0.0607	0.0606	0.0606
$\ell^{\text{true}} = 0.08$	0.0810	0.0810	0.0811
$\ell^{\text{true}} = 0.10$	—	—	0.102
$\ell^{\text{true}} = 0.12$	—	—	0.123

Table 2: *Identification of buried straight crack of half-length ℓ^{true}: estimated size ℓ^{est}, with $\boldsymbol{x}^{est} = (0.6,\ 0.48)$, i.e. closest to $\boldsymbol{x}^{true}$, in all cases shown.*

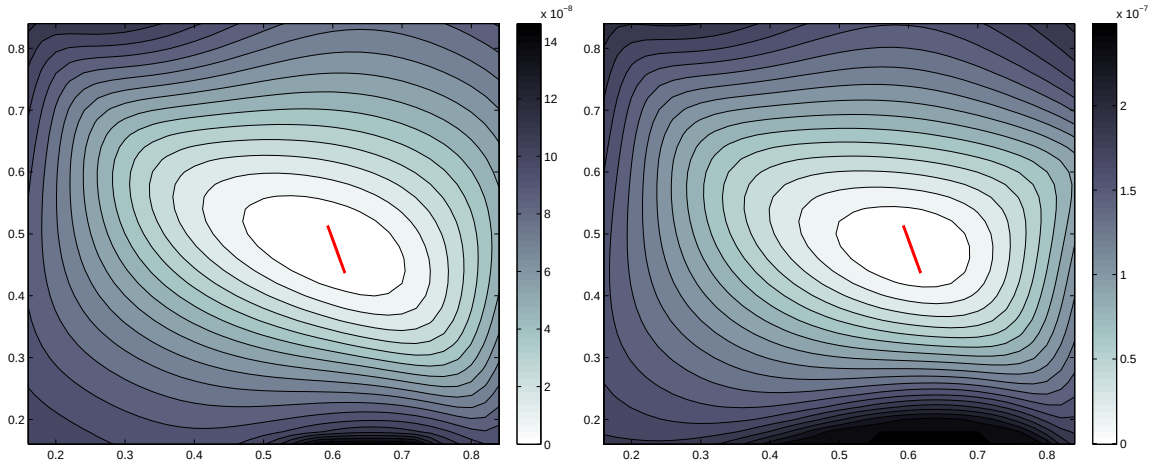

Figure 5: *Distribution of $J^{min}(\boldsymbol{z})$ over search grid* $\mathbf{G}$*, and outline of true crack, for sensor set S3, $\ell^{true} = 0.4$, $\sigma = 0$. and $M = 1$ (left) or $M = 2$ (right).*

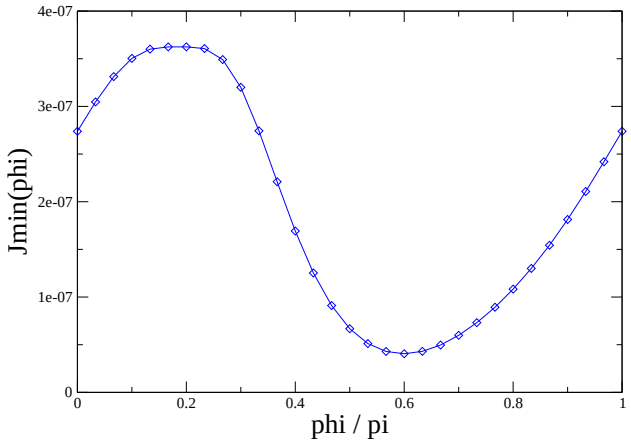

Figure 6: *Plot of $\varphi \mapsto J^{min}(\boldsymbol{z}^{est}, \varphi)$ for sensor set S1, $\ell^{true} = 0.4$ and $\sigma = 0.4$.*

The above procedure, while not currently implemented, is computationally feasible as it entails, for each sampling point, an univariate minimization. Figure 6 shows the plot of the function $\varphi \mapsto J^{\min}(\boldsymbol{z}^{\text{est}}, \varphi)$ for one of the above-presented identification cases. The correct orientation $\varphi^{\text{true}} = 3\pi/5$ is clearly seen to correspond to the minimum of the univariate function $\varphi \mapsto J^{\min}(\boldsymbol{z}^{\text{est}}, \varphi)$.

7 CONCLUSIONS

In this article, continuing previous work on higher-order topological sensitivity, a methodology for expanding to order $O(a^4)$ the perturbation undergone by a generic cost functional under the nucleation of a small trial crack of characteristic size a has been expounded, in the context of 2-D media characterized by a scalar conductivity. General formulae have been provided, where an adjoint solution is used to simplify the procedure through avoiding evaluation of higher-order topological sensitivities of field variables at locations away from the trial nucleating crack. A non-iterative approximate global crack identification procedure based on the higher-order topological sensitivity has been proposed and validated on numerical experiments. This approach is expected to perform at a computational cost much lower than that of conventional global search algorithms. The proposed methodology is generic (its main thrust in fact following [9]) and is therefore expected to yield similar expansions (and identification methodologies) for other cases, e.g. cracks in 3-D elastic solids under static or dynamic conditions. Such developments will be addressed in forthcoming investigations.

Appendix A THE CASE OF A CENTRALLY-SYMMETRIC CRACK

When $\mathcal{D}$ has central symmetry (i.e. if $\bar{\boldsymbol{\xi}} \in \mathcal{D} \Leftrightarrow -\bar{\boldsymbol{\xi}} \in \mathcal{D}$), the constant tensor $\boldsymbol{\mathcal{A}}_{21}$ defined by (54a) vanishes. Denoting by $\sigma : \ \bar{\boldsymbol{\xi}} \mapsto \sigma\bar{\boldsymbol{\xi}} \coloneqq -\bar{\boldsymbol{\xi}}$ the central-symmetry linear mapping, which is in particular such that

$$\text{(a)}\ \ \boldsymbol{n}(\sigma\bar{\boldsymbol{\xi}}) = \boldsymbol{n}(\bar{\boldsymbol{\xi}}), \qquad \text{(b)}\ \ \mathrm{d}s(\sigma\bar{\boldsymbol{\xi}}) = \mathrm{d}s(\bar{\boldsymbol{\xi}}), \tag{A.1}$$

let $\mathcal{D} = \mathcal{D}' \cup \mathcal{D}''$, with $\mathcal{D}'' = \sigma\mathcal{D}'$ and $\mathcal{D}' \cap \mathcal{D}'' = \{O\}$ (where O is the coordinate origin in $\bar{\boldsymbol{\xi}}$-space).

Lemma 7. *The following hold when the normalized crack has central symmetry: (a) solution $\boldsymbol{\mathcal{U}}_1$ is symmetric: $\boldsymbol{\mathcal{U}}_1(\sigma\bar{\boldsymbol{\xi}}) = \boldsymbol{\mathcal{U}}_1(\bar{\boldsymbol{\xi}})$, and (b) $\boldsymbol{\mathcal{A}}_{21}(\mathcal{D}) = \boldsymbol{0}$.*

Proof. Let $\boldsymbol{\mathcal{U}}_1^{\text{even}}$ and $\boldsymbol{\mathcal{U}}_1^{\text{odd}}$, the even and odd parts of $\boldsymbol{\mathcal{U}}_1$, be defined by:

$$\boldsymbol{\mathcal{U}}_1^{\text{even}}(\bar{\boldsymbol{\xi}}) = \frac{1}{2}\big(\boldsymbol{\mathcal{U}}_1(\bar{\boldsymbol{\xi}}) + \boldsymbol{\mathcal{U}}_1(\sigma\bar{\boldsymbol{\xi}})\big)\,, \qquad \boldsymbol{\mathcal{U}}_1^{\text{odd}}(\bar{\boldsymbol{\xi}}) = \frac{1}{2}\big(\boldsymbol{\mathcal{U}}_1(\bar{\boldsymbol{\xi}}) - \boldsymbol{\mathcal{U}}_1(\sigma\bar{\boldsymbol{\xi}})\big). \tag{A.2}$$

These definitions imply that

$$\boldsymbol{\mathcal{U}}_1^{\text{even}}(\sigma\bar{\boldsymbol{\xi}}) = \boldsymbol{\mathcal{U}}_1^{\text{even}}(\bar{\boldsymbol{\xi}})\,, \qquad \boldsymbol{\mathcal{U}}_1^{\text{odd}}(\sigma\bar{\boldsymbol{\xi}}) = -\boldsymbol{\mathcal{U}}_1^{\text{odd}}(\bar{\boldsymbol{\xi}}), \tag{A.3a}$$

$$\partial_{\bar{\tau}}\boldsymbol{\mathcal{U}}_1^{\text{even}}(\sigma\bar{\boldsymbol{\xi}}) = -\partial_{\bar{\tau}}\boldsymbol{\mathcal{U}}_1^{\text{even}}(\bar{\boldsymbol{\xi}})\,, \qquad \partial_{\bar{\tau}}\boldsymbol{\mathcal{U}}_1^{\text{odd}}(\sigma\bar{\boldsymbol{\xi}}) = \partial_{\bar{\tau}}\boldsymbol{\mathcal{U}}_1^{\text{odd}}(\bar{\boldsymbol{\xi}}). \tag{A.3b}$$

Now, on inserting the decomposition $\boldsymbol{\mathcal{U}}_1 = \boldsymbol{\mathcal{U}}_1^{\text{even}} + \boldsymbol{\mathcal{U}}_1^{\text{odd}}$ in integral equation (46b), writing the resulting equations for a pair of symmetrical collocation points $\bar{\boldsymbol{x}}$ and $\sigma\bar{\boldsymbol{x}}$ ($\bar{\boldsymbol{x}} \in \mathcal{D}'$), using properties (A.1a) and (A.3b), and noting that the distance function and the fundamental solution $G(\boldsymbol{r})$ defined by (33) satisfy

$$\|\sigma\bar{\boldsymbol{x}} - \bar{\boldsymbol{\xi}}\| = \|\bar{\boldsymbol{x}} - \sigma\bar{\boldsymbol{\xi}}\|\,, \qquad \boldsymbol{\nabla}G(\bar{\boldsymbol{\xi}} - \sigma\bar{\boldsymbol{x}}) = -\boldsymbol{\nabla}G(\sigma\bar{\boldsymbol{\xi}} - \bar{\boldsymbol{x}}),$$

the following pair of integral equations is arrived at:

$$\begin{aligned} &\big[\bar{\mathcal{L}}_{\mathcal{D}'}^{\text{even}}\boldsymbol{\mathcal{U}}_1^{\text{even}}\big](\bar{\boldsymbol{x}}) + \big[\bar{\mathcal{L}}_{\mathcal{D}'}^{\text{odd}}\boldsymbol{\mathcal{U}}_1^{\text{odd}}\big](\bar{\boldsymbol{x}}) = \boldsymbol{n}(\bar{\boldsymbol{x}}) \otimes \bar{\boldsymbol{x}}, \\ &\big[\bar{\mathcal{L}}_{\mathcal{D}'}^{\text{even}}\boldsymbol{\mathcal{U}}_1^{\text{even}}\big](\bar{\boldsymbol{x}}) - \big[\bar{\mathcal{L}}_{\mathcal{D}'}^{\text{odd}}\boldsymbol{\mathcal{U}}_1^{\text{odd}}\big](\bar{\boldsymbol{x}}) = \boldsymbol{n}(\bar{\boldsymbol{x}}) \otimes \bar{\boldsymbol{x}} \end{aligned} \qquad (\bar{\boldsymbol{x}} \in \mathcal{D}'), \tag{A.4}$$

with the definitions

$$\big[\bar{\mathcal{L}}_{\mathcal{D}'}^{\text{even}} f\big](\bar{\boldsymbol{x}}) = \big[\bar{\mathcal{L}}_{\mathcal{D}'} f\big](\bar{\boldsymbol{x}}) + \big[\bar{\mathcal{L}}_{\mathcal{D}'} f\big](\sigma\bar{\boldsymbol{x}}), \qquad \big[\bar{\mathcal{L}}_{\mathcal{D}'}^{\text{odd}} f\big](\bar{\boldsymbol{x}}) = \big[\bar{\mathcal{L}}_{\mathcal{D}'} f\big](\bar{\boldsymbol{x}}) - \big[\bar{\mathcal{L}}_{\mathcal{D}'} f\big](\sigma\bar{\boldsymbol{x}}).$$

On taking the difference of equations (A.4), one obtains $\big[\bar{\mathcal{L}}_{\mathcal{D}'}^{\text{odd}}\boldsymbol{\mathcal{U}}_1^{\text{odd}}\big](\bar{\boldsymbol{x}}) = \boldsymbol{0}$, i.e. $\boldsymbol{\mathcal{U}}_1^{\text{odd}}(\bar{\boldsymbol{\xi}}) = \boldsymbol{0}$ ($\boldsymbol{\mathcal{U}}_1$ is symmetric). Result (a) is thus established.

Then, using (a), result (b) follows from

$$\boldsymbol{\mathcal{A}}_{21} = \int_{\mathcal{D}} \boldsymbol{n} \otimes \bar{\boldsymbol{\xi}} \otimes \boldsymbol{\mathcal{U}}_1 \,\mathrm{d}s(\bar{\boldsymbol{\xi}}) = \int_{\mathcal{D}'} \boldsymbol{n} \otimes [\bar{\boldsymbol{\xi}} \otimes \boldsymbol{\mathcal{U}}_1(\bar{\boldsymbol{\xi}}) - \bar{\boldsymbol{\xi}} \otimes \boldsymbol{\mathcal{U}}_1(\sigma\bar{\boldsymbol{\xi}})] \otimes \boldsymbol{n} \,\mathrm{d}s(\bar{\boldsymbol{\xi}}) = \boldsymbol{0}. \qquad \square$$

Appendix B DETERMINATION OF $\mathcal{U}_1, \mathcal{U}_2$ AND ASSOCIATED CONSTANT TENSORS

On considering integral equation (34) for the case of an unbounded medium (hence $\mathcal{M}(\boldsymbol{x}, \boldsymbol{\xi}) = 0$), rescaling it for a normalized crack D_a, and noting from (12c) that $\mp p[u]$ in (34) is the flux applied to the crack faces, one finds that integral equations of the form

$$[\bar{\mathcal{L}}U](\bar{\boldsymbol{x}}) = q^{\mathrm{d}}(\bar{\boldsymbol{x}}) \tag{B.1}$$

govern solutions U to problems for infinite media containing a normalized crack $\mathcal{D}$ of the form

$$\text{(a)}\ \ k\Delta U = 0\ \ (\text{in } \mathbb{R}^2 \setminus \mathcal{D}), \quad \text{(b)}\ \ p^{\pm}[U] = \mp q^{\mathrm{d}}\ \ (\text{on } \mathcal{D}^{\pm}), \quad \text{(c)}\ \ U \to 0\ \ (\text{at infinity}), \tag{B.2}$$

where q^{d} is a prescribed flux. Moreover, one notes that problem (B.2) admits the weak formulation

$$\int_{\mathbb{R}^2 \setminus \mathcal{D}} k\boldsymbol{\nabla}U \cdot \boldsymbol{\nabla}W \,\mathrm{d}V = -\int_{\mathcal{D}} q^{\mathrm{d}} [\![W]\!] \,\mathrm{d}s \tag{B.3}$$

where W stands for any trial function defined on $\mathbb{R}^2\setminus\mathcal{D}$ and of bounded H^1 norm, a result which follows from the usual approach of multiplying (B.2a) by W, integrating by parts and plugging boundary conditions (B.2b) in the contour integral over $\mathcal{D}$.

The vector and tensor functions $\boldsymbol{\mathcal{U}}_1, \boldsymbol{\mathcal{U}}_2, \boldsymbol{\mathcal{U}}_3$ introduced in Lemma 4 are solutions to integral equations of the form (B.1), with $q^{\mathrm{d}} = \boldsymbol{n}$, $q^{\mathrm{d}} = \boldsymbol{n}\otimes\bar{\boldsymbol{x}}$ and $q^{\mathrm{d}} = \boldsymbol{n}\otimes\bar{\boldsymbol{x}}\otimes\bar{\boldsymbol{x}}$, respectively. They thus also verify the weak formulation (B.3).

Determination of $\boldsymbol{\mathcal{U}}_1, \boldsymbol{\mathcal{U}}_2, \boldsymbol{\mathcal{U}}_3$ for straight cracks. When $\mathcal{D}$ is a normalized straight crack of length 2, and using the notations of Lemma 6, the normalized integral equation (B.1) becomes

$$-\frac{1}{2\pi}\int_{-1}^{1} U'(\bar{z})\frac{\mathrm{d}\bar{z}}{\bar{z}-\bar{x}} = q^{\mathrm{d}}(\bar{x}) \qquad (-1<\bar{x}<1). \tag{B.4}$$

For polynomial right-hand sides $q^{\mathrm{d}}(\bar{x})$, the solution U is known to be of the form

$$U(\bar{z}) = (1-\bar{z}^2)^{1/2}P(\bar{z}) \implies U'(\bar{z}) = (1-\bar{z}^2)^{-1/2}\big[(1-\bar{z}^2)P'(\bar{z}) - \bar{z}P(\bar{z})\big], \tag{B.5}$$

where P is a polynomial, and can be found in practice by exploiting identity [17]

$$\int_{-1}^{1}(1-\bar{z}^2)^{-1/2}T_n(\bar{z})\frac{\mathrm{d}\bar{z}}{\bar{z}-\bar{x}} = \pi U_{n-1}(\bar{x}), \tag{B.6}$$

where T_n and U_n are Chebyshev polynomials of the first and second kind, respectively [1]. In particular, noting that $U_0(\bar{z})=1,\ U_1(\bar{z})=2\bar{z},\ U_1(\bar{z})=4\bar{z}^2-1$, the right-hand sides of equations (46a-c) can be expressed as

$$\boldsymbol{n} = U_0(\bar{x})\boldsymbol{n}, \quad \boldsymbol{n}\otimes\bar{\boldsymbol{x}} = \frac{1}{2}U_1(\bar{x})\boldsymbol{n}\otimes\boldsymbol{\tau}, \quad \boldsymbol{n}\otimes\bar{\boldsymbol{x}}\otimes\bar{\boldsymbol{x}} = \frac{1}{4}[U_2+U_0](\bar{x})\boldsymbol{n}\otimes\boldsymbol{\tau}\otimes\boldsymbol{\tau}. \tag{B.7}$$

Tensor functions $\boldsymbol{\mathcal{U}}_1, \boldsymbol{\mathcal{U}}_2, \boldsymbol{\mathcal{U}}_3$ are the solutions to the normalized integral equation (B.4) with right-hand sides given by (B.7). Noting that $T_1(\bar{z})=\bar{z},\ T_2(\bar{z})=2\bar{z}-1,\ T_3(\bar{z})=4\bar{z}^3-3\bar{z}$, one readily checks with the help of (B.5), (B.6) and (B.7) that $\boldsymbol{\mathcal{U}}_1, \boldsymbol{\mathcal{U}}_2, \boldsymbol{\mathcal{U}}_3$ respectively correspond to $P(\bar{z})=2$, $P(\bar{z})=\bar{z}$ and $P(\bar{z})=(2\bar{z}^2+1)/3$ in (B.5) and are thus given by (61a-c).

Appendix C ANALYTICAL EXAMPLE: CIRCULAR DOMAIN WITH CENTRAL CRACK

The goal of this appendix is to find analytical results in terms of expanding solutions and cost functions with respect to a for the case of a central crack in a disk-shaped domain whose boundary is subjected to a prescribed flux, which provide checks and illustrations for the general results of Secs 4, 5. Letting $\Omega = \{(r,\theta)\,\big|\,r<b\}$ (where (r,θ) are polar coordinates) denote the disk of radius b centered at the origin, the cracked domain Ω_a corresponds to a central crack defined by $-a<\xi_1<a$. Here again, $\bar{x}_1, \bar{\xi}_1$ will simply be denoted $\bar{x}, \bar{\xi}$ for simplicity.

Green's functions for Neumann problems. The relevant Green's function $\mathcal{G}(\boldsymbol{x},\boldsymbol{\xi})$ is defined by (32) and (33) with

$$G_{\mathrm{C}}(\boldsymbol{x},\boldsymbol{\xi}) = \frac{1}{2\pi}\mathrm{Log}\Big(\frac{1}{R}\frac{b}{\|\boldsymbol{x}\|}\Big), \qquad \text{with} \quad R=\|\boldsymbol{R}\|,\ \ \boldsymbol{R}=\boldsymbol{\xi}-(b^2/\|\boldsymbol{x}\|^2)\boldsymbol{x}. \tag{C.1}$$

The respective boundary condition satisfied on $S=\{(r,\theta)\,\big|\,r=b\}$ by $\mathcal{G}$ is:

$$\mathcal{H}(\boldsymbol{x},\boldsymbol{\xi}) = -\frac{1}{2\pi b} \qquad (\boldsymbol{\xi}\in S). \tag{C.2}$$

On evaluating analytically $\boldsymbol{\nabla}_{12}G_{\mathrm{C}}$ by straightforward differentiation, one finds:

$$\boldsymbol{\nabla}_2 G_{\mathrm{C}}(\boldsymbol{x},\boldsymbol{\xi}) = -\frac{1}{2\pi}\frac{\boldsymbol{R}}{R^2},$$
$$\boldsymbol{\nabla}_{12} G_{\mathrm{C}}(\boldsymbol{x},\boldsymbol{\xi}) = -\frac{1}{2\pi}\Big[\frac{1}{R^2}\boldsymbol{I} - \frac{2}{R^4}\boldsymbol{R}\otimes\boldsymbol{R}\Big]\cdot\boldsymbol{\nabla}_1\boldsymbol{R},$$

with

$$\boldsymbol{\nabla}_1 \boldsymbol{R} = \frac{b^2}{\|\boldsymbol{x}\|^4}\big[2\boldsymbol{x}\otimes\boldsymbol{x} - \|\boldsymbol{x}\|^2\boldsymbol{I}\big].$$

Setting $\boldsymbol{x} = \boldsymbol{\xi} = \boldsymbol{z}$ for an arbitrary sampling point in Ω, one has in particular

$$\boldsymbol{\nabla}_{12x} G_{\mathrm{C}}(\boldsymbol{z},\boldsymbol{z}) = \frac{1}{2\pi}\frac{b^2}{(b^2-\|\boldsymbol{z}\|^2)^2}\boldsymbol{I}. \tag{C.3}$$

Free field. Three situations (a), (b), (c) are considered, differing by the applied flux p^{d}; they are defined as follows in terms of the boundary data p^{d} and induced free fields $u^{(a,b,c)}$:

$$\begin{aligned}
&p^{\mathrm{d}} = (ku_0/b)\sin\theta \quad (\text{on } S), && u^{(a)}(r,\theta) = \frac{u_0 r}{b}\sin\theta,\\
&p^{\mathrm{d}} = 2(ku_0/b)\sin 2\theta \quad (\text{on } S), && u^{(b)}(r,\theta) = \frac{u_0 r^2}{b^2}\sin 2\theta,\\
&p^{\mathrm{d}} = 3(ku_0/b)\sin 3\theta \quad (\text{on } S), && u^{(c)}(r,\theta) = \frac{u_0 r^3}{b^3}\sin 3\theta.
\end{aligned} \tag{C.4}$$

The gradients of $u^{(a,b,c)}$ at the sampling point $\boldsymbol{z} = (0,0)$ are given by

$$\begin{aligned}
\boldsymbol{\nabla}u^{(a)}(\boldsymbol{z}) &= \frac{u_0}{b}\boldsymbol{n}, & \boldsymbol{\nabla}u^{(b)}(\boldsymbol{z}) &= \boldsymbol{0},\\
\boldsymbol{\nabla}^2u^{(a)}(\boldsymbol{z}) &= \boldsymbol{0}, & \boldsymbol{\nabla}^2u^{(b)}(\boldsymbol{z}) &= \frac{2u_0}{b^2}(\boldsymbol{\tau}\otimes\boldsymbol{n}+\boldsymbol{n}\otimes\boldsymbol{\tau}),\\
\boldsymbol{\nabla}^3u^{(a)}(\boldsymbol{z}) &= \boldsymbol{0}, & \boldsymbol{\nabla}^3u^{(b)}(\boldsymbol{z}) &= \boldsymbol{0},\\
\boldsymbol{\nabla}u^{(c)}(\boldsymbol{z}) &= \boldsymbol{0},\\
\boldsymbol{\nabla}^2u^{(c)}(\boldsymbol{z}) &= \boldsymbol{0},\\
\boldsymbol{\nabla}^3u^{(c)}(\boldsymbol{z}) &= \frac{6u_0}{b^3}(\boldsymbol{\tau}\otimes\boldsymbol{\tau}\otimes\boldsymbol{n}+\boldsymbol{\tau}\otimes\boldsymbol{n}\otimes\boldsymbol{\tau}+\boldsymbol{n}\otimes\boldsymbol{\tau}\otimes\boldsymbol{\tau}-\boldsymbol{n}\otimes\boldsymbol{n}\otimes\boldsymbol{n}).
\end{aligned} \tag{C.5}$$

Moreover, the flux on the crack faces is such that (using the same convention as in Lemma 1)

$$p[u^{(a)}] = u_0/b, \qquad p[u^{(b)}] = (2u_0/b^2)a\bar{x}, \qquad p[u^{(c)}] = (3u_0/b^3)a^2\bar{x}^2. \tag{C.6}$$

Asymptotic expansion on the crack. For $\boldsymbol{x},\boldsymbol{\xi}\in D_a$, one has $\boldsymbol{x} = a\bar{x}\boldsymbol{\tau}$, $\boldsymbol{\xi} = a\bar{\xi}\boldsymbol{\tau}$, so that

$$R^2 = \frac{1}{a^2\bar{x}^2}(a^2\bar{\xi}\bar{x}-b^2)^2, \qquad \boldsymbol{R}\cdot\boldsymbol{n} = 0, \qquad \boldsymbol{\nabla}_1\boldsymbol{R}\cdot\boldsymbol{n} = -\frac{b^2}{(a\bar{x})^2}\boldsymbol{n},$$

$$\boldsymbol{\tau}\cdot\boldsymbol{\nabla}_2 G_{\mathrm{C}}(\boldsymbol{x},\boldsymbol{\xi}) = -\frac{1}{2\pi a}\frac{1}{\bar{\xi}-\bar{x}}$$

$$\boldsymbol{n}\cdot\boldsymbol{\nabla}_{12} G_{\mathrm{C}}(\boldsymbol{x},\boldsymbol{\xi})\cdot\boldsymbol{n} = \frac{1}{2\pi}\frac{b^2}{(a^2\bar{\xi}\bar{x}-b^2)^2}.$$

Upon noting that

$$\frac{b^2}{(a^2\bar{\xi}\bar{x}-b^2)^2} = -\frac{b^2}{a^2\bar{x}}\frac{d}{d\bar{\xi}}\frac{1}{a^2\bar{\xi}\bar{x}-b^2},$$

integral equation (34) then becomes

$$-\frac{1}{2\pi a}\int_{-1}^{1}\frac{\mathrm{d}\bar{z}}{\bar{z}-\bar{x}}\phi_a'(\bar{z}) - \frac{1}{2\pi}\frac{b^2}{a\bar{x}}\int_{-1}^{1}\frac{\mathrm{d}\bar{z}}{a^2\bar{\xi}\bar{x}-b^2}\phi_a'(\bar{z}) = p[u](a\bar{x}).$$

Seeking $\phi_a(\bar{\xi})$ in the form

$$\phi_a(\bar{\xi}) = \sum_{n\geq 0}\alpha_n(1-\bar{\xi}^2)^{1/2}U_n(\bar{\xi}) \implies \phi_a'(\bar{\xi}) = -\sum_{n\geq 0}\alpha_n(1-\bar{\xi}^2)^{-1/2}(n+1)T_{n+1}(\bar{\xi})$$

and invoking identity (B.6), the above integral equation takes the form

$$\sum_{n\geq 0}(n+1)\Big[U_n(\bar{x}) - \frac{\pi}{2}K_n(\bar{x})\Big]\alpha_n = 2ap[u](a\bar{x}), \tag{C.7}$$

having set

$$K_n(\bar{x}) = -\frac{2b^2}{\pi^2\bar{x}}\int_{-1}^{1}\frac{\mathrm{d}\bar{z}}{a^2\bar{\xi}\bar{x} - b^2}(1-\bar{\xi}^2)^{-1/2}T_{n+1}(\bar{\xi}).$$

Using the change of variable $\bar{\xi} = \cos u$ and recalling that $T_{n+1}(\bar{\xi}) = \cos(n+1)u$, one has

$$K_n(\bar{x}) = \frac{2}{\pi^2\bar{x}}\int_0^{\pi}\frac{\cos(n+1)u}{1-(a^2\bar{x}/b^2)\cos u}\,\mathrm{d}u. \tag{C.8}$$

For sufficiently small a, one has $|(a^2\bar{x}/b^2)\cos u| < 1$, in which case the expansion

$$\frac{1}{1-(a^2\bar{x}/b^2)\cos u} = \sum_{m\geq 0}(a^2\bar{x}/b^2)^m\cos^m u$$

can be substituted into (C.8) to obtain

$$K_n(\bar{x}) = \frac{2a^2}{\pi^2 b^2}\sum_{m\geq 0}\Big(\frac{a^2\bar{x}}{b^2}\Big)^m\int_0^{\pi}\cos(n+1)u\cos^{m+1}u\,\mathrm{d}u,$$

having used that $\int_0^{\pi}\cos(n+1)u\,\mathrm{d}u = 0$. To evaluate $K_n(\bar{x})$ to order $O(a^3)$, one needs only consider the case $m = 0$ in the above series. Noting that

$$\int_0^{\pi}\cos(n+1)u\cos u\,\mathrm{d}u = \frac{\pi}{2}\delta_{n0},$$

one obtains

$$K_0(\bar{x}) = \frac{a^2}{\pi b^2} + o(a^3), \qquad K_n(\bar{x}) = o(a^3)\ \ (n\geq 1). \tag{C.9}$$

Now, one observes (by virtue of the orthogonality property $\langle U_m, U_n\rangle = (\pi/2)\delta_{mn}$ of the Chebyshev polynomials U_n and since $U_0(\bar{x}) = 1$) that

$$\langle U_m, K_0\rangle = \frac{a^2}{\pi b^2}\langle U_m, U_0\rangle + o(a^3) = \frac{a^2}{2b^2}\delta_{m0} + o(a^3).$$

Multiplying (C.7) by $(1-\bar{x}^2)^{1/2}U_m(\bar{x})$, integrating the result over $-1 \geq \bar{x} \geq 1$, invoking the above-mentioned orthogonality property and using expansions (C.9), one obtains an infinite matrix equation for $\{\tilde{\alpha}\} = \{(n+1)\alpha_n, n\geq 0\}$ of the form

$$\frac{\pi}{2}[I-K]\{\tilde{\alpha}\} = a\{y\}, \tag{C.10}$$

where $[I]$ is the (infinite) identity matrix, the infinite matrix $[K]$ is such that

$$[K] = \frac{a^2}{2b^2}\{e\}\{e\}^{\mathrm{T}} + o(a^3) \tag{C.11}$$

(where $\{e\}$ is the infinite vector such that $e_m = \delta_{m0}$) and the infinite vector $\{y\} = \{y_m, m\geq 0\}$ is defined by

$$y_m = 2\langle U_m, p[u](a\bar{x})\rangle.$$

Since $[K] = O(a^2)$, one has for sufficiently small a

$$[I-K]^{-1} = [I+K] + o(a^3),$$

so that the solution to the infinite matrix equation (C.10) is, by virtue of (C.11), given by

$$\{\tilde{\alpha}\} = \frac{2a}{\pi}\{y\} + \frac{a^3}{\pi b^2} y_0 \{e\}.$$

For the above-defined reference fields $u^{(a)}$, $u^{(b)}$ and $u^{(,f)}$, the non-zero values of y_m are found from (C.6) to be

$$y_0^{(a)} = \frac{\pi u_0}{b}, \qquad y_1^{(b)} = \frac{\pi u_0}{b^2} a, \qquad y_0^{(c)} = y_2^{(c)} = \frac{3\pi u_0}{4b^3} a^2. \tag{C.12}$$

The only non-zero entries of $\{\alpha\}$ for these cases are thus given by

$$\alpha_0^{(a)} = \frac{2u_0}{b} a + \frac{u_0}{b^3} a^3 + o(a^3), \qquad \alpha_1^{(b)} = \frac{u_0}{b^2} a^2 + o(a^3), \qquad \alpha_0^{(c)} = 3\alpha_2^{(c)} = \frac{3u_0}{2b^3} a^3 + o(a^3). \tag{C.13}$$

Asymptotic expansion on the external boundary. Let $\boldsymbol{x}$ now denote a point on S. Since (C.1) implies that $G_{\mathrm{C}}(\boldsymbol{x}, \boldsymbol{\xi}) = G(\boldsymbol{\xi} - \boldsymbol{x})$ for $\boldsymbol{x} \in S$ (for which $\|\boldsymbol{x}\| = b$), the integral representation (28) reduces to

$$u_a(\boldsymbol{x}) - u(\boldsymbol{x}) = 2\int_{D_a} H(\boldsymbol{x}, \boldsymbol{\xi}) \phi_a(\boldsymbol{\xi}) \, \mathrm{d}s(\boldsymbol{\xi}) = 2a \int_{-1}^{1} H(\boldsymbol{x}, a\bar{\boldsymbol{\xi}}) \phi_a(\bar{\boldsymbol{\xi}}) \, \mathrm{d}s(\bar{\boldsymbol{\xi}}) \quad (\boldsymbol{x} \in S). \tag{C.14}$$

The expansion of (C.14) to order $O(a^4)$ is sought.

Letting θ denote the angular polar coordinate of $\boldsymbol{x} \in S$, one finds

$$H(\boldsymbol{x}, \boldsymbol{\xi}) = -\frac{1}{2\pi} \frac{(\boldsymbol{\xi} - \boldsymbol{x}) \cdot \boldsymbol{n}}{\|\boldsymbol{\xi} - \boldsymbol{x}\|^2} = \frac{1}{2\pi} \frac{\sin\theta}{\pi b} \frac{1}{1 - 2(a/b)\cos\theta\bar{\xi} + (a/b)^2 \bar{\xi}^2}.$$

Since $\mathrm{d}s(\boldsymbol{\xi})$ and ϕ_a both are of order $O(a)$, the above formula needs to be expanded only to order $O(a^2)$ for the present purposes. One finds

$$\begin{aligned} H(\boldsymbol{x}, \boldsymbol{\xi}) &= \frac{1}{2\pi} \frac{\sin\theta}{\pi b} \Big[1 + 2(a/b)\cos\theta\bar{\xi} + (a/b)^2 \big(4\cos^2\theta - 1\big)\bar{\xi}^2 \Big] + o(a^2), \\ &= \frac{1}{2\pi} \frac{\sin\theta}{\pi b} \Big[U_0(\bar{\xi}) + (a/b)\cos\theta U_1(\bar{\xi}) + (a/2b)^2 \big(4\cos^2\theta - 1\big) \big[U_0(\bar{\xi}) + U_2(\bar{\xi}) \big] \Big] + o(a^2). \end{aligned}$$

Moreover, one has

$$\phi_a(\bar{\boldsymbol{\xi}}) = (1 - \bar{\xi}^2)^{1/2} \big[\alpha_0 U_0(\bar{\xi}) + \alpha_1 U_1(\bar{\xi}) + \alpha_2 U_2(\bar{\xi}) \big] + o(a^3),$$

with $\alpha_0 = O(a)$, $\alpha_1 = O(a^2)$ and $\alpha_2 = O(a^3)$. Plugging the above expressions of $H(\boldsymbol{x}, \boldsymbol{\xi})$ and $\phi_a(\bar{\boldsymbol{\xi}})$ into (C.14), evaluating the resulting integral by using again the orthogonality property of the Chebyshev polynomials, leaving out all $o(a^4)$ contributions and rearranging the result, one obtains

$$u_a(\boldsymbol{x}) = u(\boldsymbol{x}) + \frac{a\sin\theta}{2b}\alpha_0 + \frac{a^2 \sin 2\theta}{4b^2}\alpha_1 + \frac{a^3 \sin 3\theta}{8b^3}\alpha_0 + o(a^4) \qquad (\boldsymbol{x} \in S). \tag{C.15}$$

Cost function expansion. As an example, consider the potential energy for the Neumann problem

$$E(u_a) = -\frac{1}{2} \int_S p^{\mathrm{d}} u_a \, \mathrm{d}s.$$

For the three states defined by the boundary data (C.4), the relevant coefficients α_n are given by (C.13) so that expansion (C.15) yields

$$E(u_a^{(a)}) = -\pi u_0^2 \Big(\frac{1}{2} + \frac{a^2}{2b^2} + \frac{a^4}{4b^4} \Big) + o(a^4), \tag{C.16a}$$

$$E(u_a^{(b)}) = -\pi u_0^2 \Big(1 + \frac{a^4}{4b^4} \Big) + o(a^4), \tag{C.16b}$$

$$E(u_a^{(c)}) = -\frac{3}{2}\pi u_0^2 + o(a^4). \tag{C.16c}$$

An evaluation of expressions (52a,c) of coefficients $\mathcal{T}_2, \mathcal{T}_4$, using (C.3) for $\boldsymbol{z} = (0, 0)$ together with formulae (C.5) and noting that $\hat{u} = -u/2$ by virtue of (16), yields $O(a^4)$ expansions of $E(u_a^{(a,b,c)})$ that coincide with the above results (C.16a–c). These special cases thus corroborate Proposition 1.

ACKNOWLEDGEMENTS

The author thanks both anonymous referees for their careful and thorough reading of the manuscript and the useful remarks they made, which permitted substantial improvements in the final version of this article.

REFERENCES

[1] ABRAMOWITZ, M., STEGUN, I. *Handbook of Mathematical Functions*. Dover Publications, New York (1972).

[2] AMMARI, H., KANG, H. *Reconstruction of small inhomogeneities from boundary measurements*. Lecture Notes in Mathematics 1846. Springer-Verlag (2004).

[3] AMSTUTZ, S. Sensitivity analysis with respect to a local perturbation of the material property. *Asymptotic Analysis*, **49**:87–108 (2006).

[4] AMSTUTZ, S., HORCHANI, I., MASMOUDI, M. Crack detection by the topological gradient method. *Control and Cybernetics*, **34**:81–101 (2005).

[5] ANDRIEUX, S., BEN ABDA, A. Identification of planar cracks by complete overdetermined data : inversion formulae. *Inverse Problems*, **12**:553–563 (1996).

[6] BEN ABDA, A., HASSINE, M., JAOUA, M., MASMOUDI, M. Topological sensitivity analysis for the location of small cavities in Stokes flow. *SIAM J. Contr. Opt.*, **48**:2871–2900 (2009).

[7] BONNET, M. *Boundary Integral Equations Methods for Solids and Fluids*. John Wiley and Sons (1999).

[8] BONNET, M. Inverse acoustic scattering by small-obstacle expansion of misfit function. *Inverse Problems*, **24**:035022 (2008).

[9] BONNET, M. Higher-order topological sensitivity for 2-D potential problems. Application to fast identification of inclusions. *Int. J. Solids Struct.*, **46**:2275–2292 (2009).

[10] BONNET, M., GUZINA, B. B. Sounding of finite solid bodies by way of topological derivative. *Int. J. Num. Meth. Eng.*, **61**:2344–2373 (2004).

[11] CARPIO, A., RAPÚN, M. L. Solving inhomogeneous inverse problems by topological derivative methods. *Inverse Problems*, **24**:045014 (2008).

[12] CÉA, J., GARREAU, S., GUILLAUME, P., MASMOUDI, M. The shape and topological optimization connection. *Comp. Meth. Appl. Mech. Eng.*, **188**:703–726 (2001).

[13] CHEN, G., ZHOU, J. *Boundary element methods*. Academic Press (1992).

[14] ESCHENAUER, H. A., KOBELEV, V. V., SCHUMACHER, A. Bubble method for topology and shape optimization of structures. *Structural Optimization*, **8**:42–51 (1994).

[15] FEIJÓO, G. R. A new method in inverse scattering based on the topological derivative. *Inverse Problems*, **20**:1819–1840 (2004).

[16] GARREAU, S., GUILLAUME, P., MASMOUDI, M. The topological asymptotic for PDE systems: the elasticity case. *SIAM J. Contr. Opt.*, **39**:1756–1778 (2001).

[17] GRADSHTEYN, I. S., RYZHIK, I. M. *Tables of integrals, series and products*. Academic Press (1980).

[18] GUZINA, B. B., BONNET, M. Topological derivative for the inverse scattering of elastic waves. *Quart. J. Mech. Appl. Math.*, **57**:161–179 (2004).

[19] GUZINA, B. B., CHIKICHEV, I. From imaging to material identification: a generalized concept of topological sensitivity. *J. Mech. Phys. Solids*, **55**:245–279 (2007).

[20] HAUG, E. J., CHOI, K. K., KOMKOV, V. *Design Sensitivity Analysis of Structural Systems*. Academic Press (1986).

[21] MALCOLM, A., GUZINA, B. On the topological sensitivity of transient acoustic fields. *Wave Motion*, **45**:821–834 (2008).

[22] MASMOUDI, M., POMMIER, J., SAMET, B. The topological asymptotic expansion for the Maxwell equations and some applications. *Inverse Problems*, **21**:547–564 (2005).

[23] MAZ'YA, V., NAZAROV, S. A., PLAMENEVSKII, B. A. *Asymptotic theory of elliptic boundary value problems under a singular perturbation of the domains (vols. 1 and 2)*. Birkhaüser (2000).

[24] MICHALEWICZ, Z., FOGEL, D. B. *How to solve it: modern heuristics*. Springer-Verlag (2004).

[25] ROCHA DE FARIA, J, NOVOTNY, A. A., FEIJÓO, R. A., TAROCO, E. First- and second-order topological sensitivity for inclusions. *Inverse Problems in Sciences and Engineering*, **17**:665–679 (2009).

[26] SCHUMACHER, A. *Topologieoptimierung von Bauteilstrukturen unter Verwendung von Lochpositionierungskriterien*. Ph.D. thesis, Univ. of Siegen, Germany (1995).

[27] SOKOLOWSKI, J., ZOLESIO, J. P. *Introduction to shape optimization. Shape sensitivity analysis*, vol. 16 of *Springer series in Computational Mathematics*. Springer-Verlag (1992).

[28] TARANTOLA, A. *Inverse problem theory and methods for model parameter estimation*. SIAM (2005).